Facies (2023) 69:8
https://doi.org/10.1007/s10347-023-00666-7

ORIGINAL ARTICLE

Stratigraphical, microfacies, and ichnological characteristics and depositional environments of the Permo–Carboniferous Aheimer Formation, western side of the Gulf of Suez, Egypt

Ahmed A. El-Refaiy[1] · Ahmed M. El-Sabbagh[1] · Magdy M. El Hedeny[1] · Ahmed S. Mansour[1] · Ahmed N. El-Barkooky[2]

Received: 31 October 2022 / Accepted: 10 April 2023 / Published online: 25 April 2023

Abstract
The palaeoenvironments of the upper Palaeozoic succession in the eastern foot slopes of the Northern Galala Plateau, west of the Gulf of Suez, Egypt, are interpreted based on a detailed study of the sequence-stratigraphic framework, sedimentary facies and trace fossils. The upper Carboniferous–lower Permian Aheimer Formation has been studied in its type section exposed in Wadi Aheimer. Three unconformities bound four 3rd-order depositional sequences, including the upper Carboniferous DS NG 1, and the lower Permian DS NG 2–4. These sequences are correlated with their counterparts on the North African and Arabian plates. The sedimentary facies characteristics indicate palaeoenvironments ranging from fluvial, estuarine, intertidal, shallow subtidal, shoreface to offshore transitional settings. The abundant and diverse ichno-assemblages are composed of horizontal, vertical and sub-vertical traces. At least 26 ichnotaxa have been identified, representing suites of the *Glossifungites*, proximal *Cruziana*, and proximal-archetypal *Cruziana* ichnofacies. Ichnofabric analysis revealed three distinct ichnofabrics: *Tisoa*, *Schaubcylindrichnus* and *Zoophycos* ichnofabrics. The trace and body fossil distribution and trophic structure of some of the recorded faunal assemblages confirm relatively stable and low-stress shallow-marine environments. In contrast, the trophic structure of some other assemblages indicates the influence of particular environmental parameters, including substrate consistency, bathymetry, water energy, productivity, rate of sedimentation, salinity and oxygen availability. The integrated results indicate that the sequences were formed during an interval dominated by different perturbations that resulted in a wide spectrum of depositional features. Moreover, evidence for Carboniferous–Permian glaciation is tentatively established in North Egypt but require further investigations.

Keywords Sequence stratigraphy · Microfacies · Ichnofacies · Palaeoenvironments · Permo–Carboniferous · Egypt

Introduction

Of the upper Palaeozoic of NE Egypt, the Permo-Carboniferous rocks occur on both sides of the Gulf of Suez, including the Northern Galala Plateau (NGP), Wadi Araba, the Southern Galala Plateau and west-central Sinai (Said 1962, 1971; Abdallah and Adindani 1963; Omara 1965; Issawi and Jux 1982; Kora 1984, 1998; Bandel and Kuss 1987; Klitzsch 1990; Klitzsch et al. 1990; Darwish 1992; El-Barkooky 1994; Issawi et al. 1999; Afify et al. 2023). As a consequence, different lithostratigraphic schemes have been proposed to describe the Permo-Carboniferous deposits in NE Egypt (Table 1) and the correlations of these successions in that region remain a debatable issue.

Carboniferous–Permian rocks crop out in the eastern foot slopes of the NGP, west of the Gulf of Suez, Egypt (Fig. 1a–c), forming a remarkable narrow strip of dark-coloured sediments. These strata represent the oldest rock units in this region, underlying different horizons of the Permo–Triassic, Jurassic and lower Cretaceous sandstones (e.g., Said 1962, 1990; Abdallah and Adindani 1963; Issawi et al. 1999). Stratigraphical, sedimentological and palaeontological studies of these upper Palaeozoic deposits have been undertaken for over a hundred years (Schweinfurth 1885;

✉ Ahmed M. El-Sabbagh
ah.elsabbagh@alexu.edu.eg; ah.elsabbagh@gmail.com

[1] Department of Geology, Faculty of Science, Alexandria University, Alexandria 21568, Egypt

[2] Department of Geology, Faculty of Science, Cairo University, Giza 12613, Egypt

Table 1 Different lithostratigraphic schemes used for the upper Palaeozoic–Triassic sedimentary succession in both sides of the Gulf of Suez (GOS) region

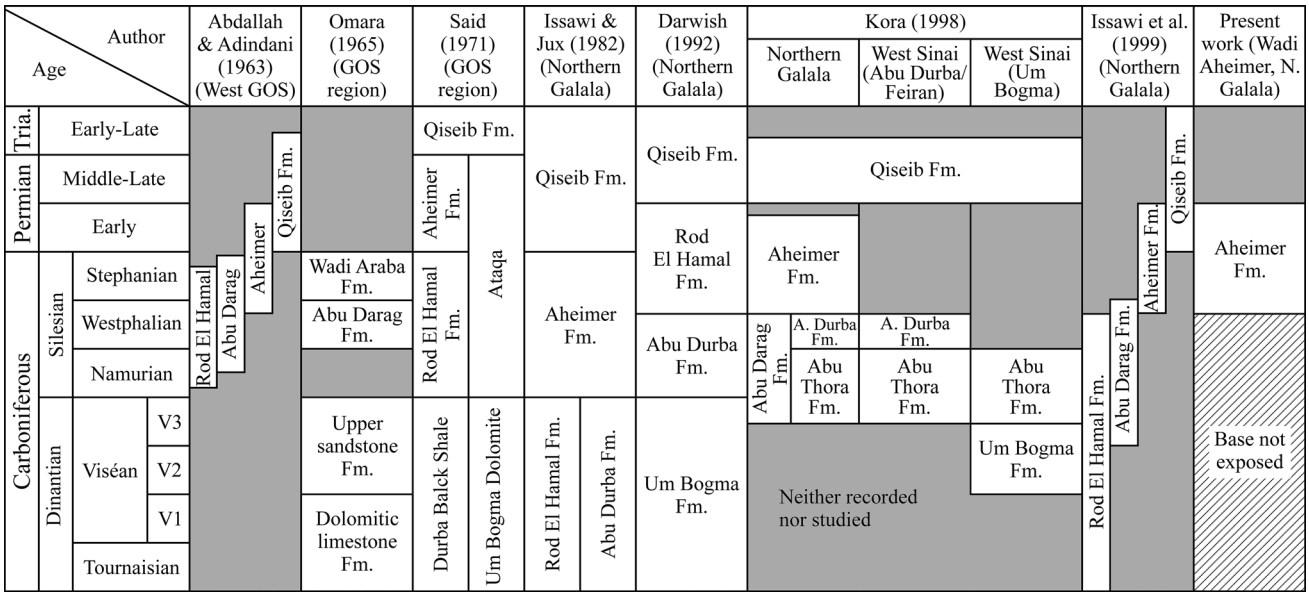

Nakkady 1955; Kostandi 1959; Abdallah and Adindani 1963; Issawi and Jux 1982; Bandel and Kuss 1987; Kora and Mansour 1992; El-Barkooky 1994; Kora 1998). The successions record fluvial to marginal-marine depositional systems (e.g., Bandel and Kuss 1987) that developed on the southwestern margin of the Palaeo-Tethys Ocean (Fig. 1d) (Scotese 2013). In general, siliciclastic deposits dominate these successions, intercalated with minor carbonates (Abdallah and Adindani 1963; Bandel and Kuss 1987). Deposition was controlled mainly by relative sea-level fluctuations combined with high terrigenous influx (e.g., Bandel and Kuss 1987).

Carboniferous–Permian deposits of the eastern side of the NGP contain a sporadic and moderately to poorly-preserved macro-invertebrate fauna, including brachiopods, bivalves, crinoids, rugose corals and bryozoans (Abdallah and Adindani 1963; Herbig and Kuss 1988; Kora and Mansour 1992; Kora 1998). In addition, these sediments yield a variety of microfaunal (foraminifera and conodonts) and floral associations (Omara and Vangerow 1965; Said and Eissa 1969; Bandel and Kuss 1987; Lejal-Nicol 1990), studied mostly from taxonomic and palaeobiogeographic points of view.

The Carboniferous–Permian sediments of the eastern side of the NGP are highly burrowed (Abdallah and Adindani 1963; Bandel and Kuss 1987; Kora and Mansour 1992; El-Barkooky 1994), representing relatively diverse ichno-assemblages. However, no study has yet focused on the analysis of the trace fossils in this area, which in turn has led to a generalized lack of detailed facies analysis along with palaeoenvironmental interpretations. Therefore, the present study aims to (1) interpret the environmental conditions that prevailed during deposition of the Carboniferous–Permian succession exposed in the eastern side of the NGP based on description of its sequence-stratigraphic framework, litho- and ichno- facies, and (2) discuss the various factors controlling the occurrence and distribution of the identified trace fossils. The present work is based on the succession exposed in the Wadi Aheimer area (29°30′38.52"N, 32°23′51.46"E), about 19 km SSE of Ain Sukhna and about 6 km NW of Bir Abu Darag along the Suez-Gharib road, in the northern Eastern Desert of Egypt (Fig. 1b, c).

Geological setting

During Palaeozoic times, North Africa was located on the southern margin of the Palaeo-Tethys Ocean (Fig. 1d; Guiraud et al. 2001, 2005; Scotese 2013). The assembly of Pangaea in the Late Palaeozoic was completed by the closing of Palaeo-Tethys along with the complex collision of Gondwana with Laurussia. During this growth of the supercontinent, several factors affected facies development across this continental shelf comprising rifting, basin sagging, compressive tectonics and sea-level fluctuations (Guiraud et al. 2005; Craig et al. 2008).

In North Africa, including Egypt, the Early Carboniferous witnessed a global rise in sea level, invading eastern Libya (e.g., Guiraud et al. 2001, 2005; Carr 2002). In the northern part of the Western Desert of Egypt, in contrast, a shallow-marine siliciclastic platform developed (e.g., Keeley 1989), passing eastwards into a mixed siliciclastic-carbonates platform (i.e., the Um Bogma Formation in

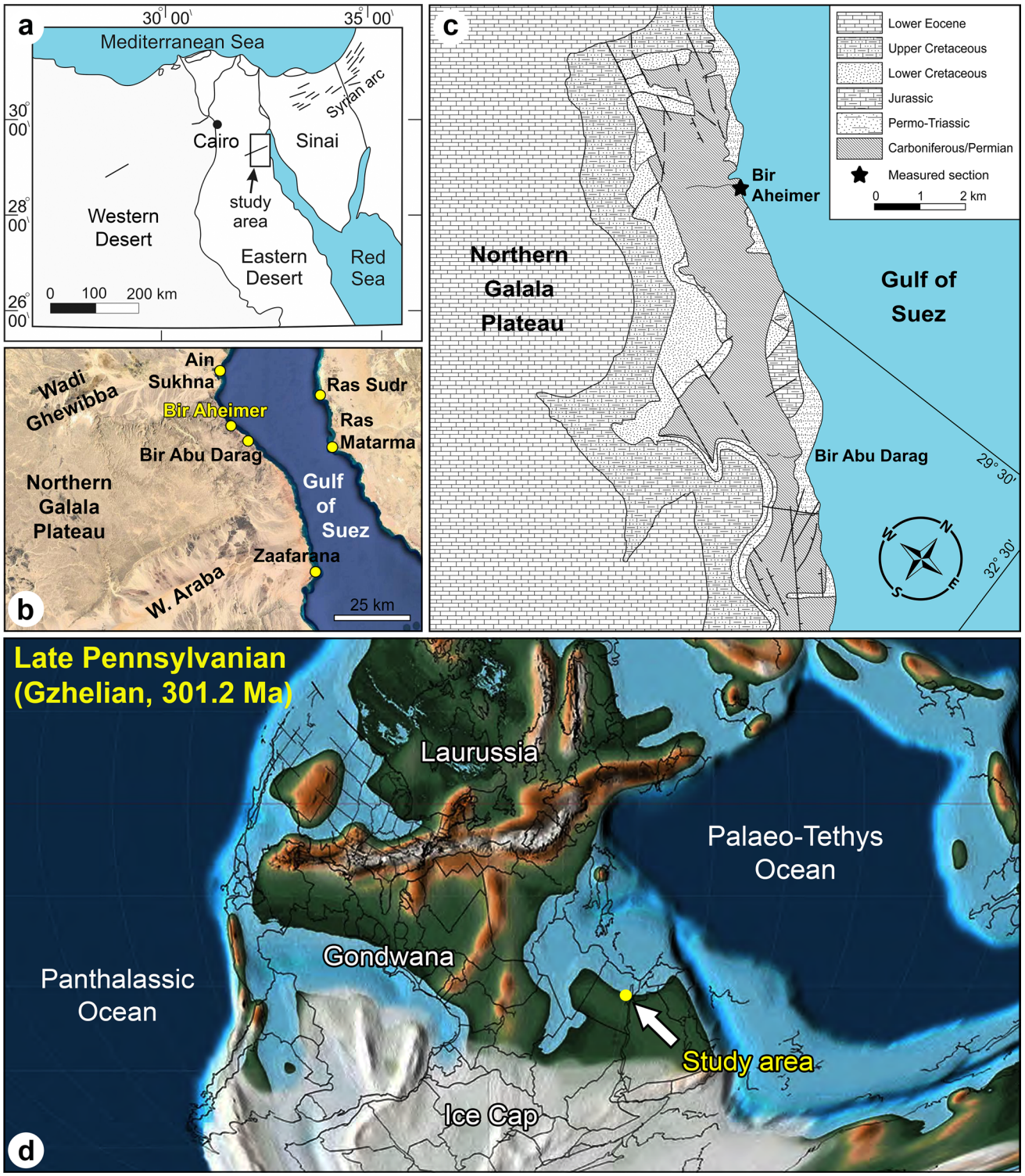

Fig. 1 Geographical and geological framework of the study area. **a** Present-day key map shows Syrian Arc and location of the Northern Galala Plateau. **b** Location of the study area. **c** Simplified geological map of the study area (after Abdallah and Adindani 1963) with indication of the measured section. **d** Palaeogeographic map shows position of the study area during the Late Pennsylvanian time (after Scotese 2013)

west-central Sinai) (Table 1; Kora 1984, 1998). A similar mixed siliciclastic-carbonate platform was developed along the northernmost margin of Algeria, Tunisia and Morocco (Guiraud et al. 2005; Craig et al. 2008). The latest Early Carboniferous registered some tectonic instability, recorded by unconformities in Egypt and Libya (Wennekers et al. 1996; Guiraud and Bosworth 1999), as well as in north-western Africa (Fabre 1988; Craig et al. 2008). During the early Westphalian, the marine conditions were restricted to north-eastern Egypt (both sides of the Gulf of Suez) and Cyrenaica (Guiraud et al. 2001, 2005; Craig et al. 2008). Sea level rose during the late Westphalian–Stephanian and a mixed carbonate siliciclastic platform fringed the North African-Arabian margin, including the western side of the Gulf of Suez (Issawi et al. 1999; Guiraud et al. 2001, 2005).

Over large areas in the Near East and North Africa, including the study area, a major unconformity marks the Carboniferous/Permian transition (Gvirtzman and Weissbrod 1984; Wennekers et al. 1996; Kora 1998; Guiraud et al. 2001, 2005; Craig et al. 2008), a consequence of uplift during the main phase of the Hercynian Orogeny. During the Early Permian, rift basins formed along the northern margins of Africa were filled by thick continental (Morocco–Algeria), mixed (Egypt), or marine sediments (S Tunisia–NW Libya) (Guiraud et al. 2005; Craig et al. 2008). These rifting events increased through the Permian (Guiraud et al. 2005), whereas subsidence affected the eastern Mediterranean margin in conjunction with the opening of the Neo-Tethys Ocean (e.g., Stampfli and Borel 2002).

The opening of the Atlantic Ocean in Triassic to Early Cretaceous times led to important extensional phases in North Africa (Craig et al. 2008 and references therein). During the Late Cretaceous and in conjunction with the onset of rifting in the northern North Atlantic and the collision between the African and European plates, a compressional regime (i.e., Alpine compression) dominated North Africa, including Egypt, and resulted in further folding, thrusting, intra-plate inversion and uplift (Maurin and Guiraud 1993; Guiraud et al. 2001, 2005; Craig et al. 2008). During Oligo–Miocene times, the north-eastern corner of Africa was affected by a major rifting phase that led to the development of the Red Sea, Gulf of Suez and Gulf of Aqaba rift systems (Meshref 1990; Patton et al. 1994; Guiraud et al. 2001, 2005).

The sedimentary succession of the NGP consists of upper Palaeozoic to lower Cretaceous siliciclastics and upper Cretaceous–Palaeogene carbonates (Said 1962; Abdallah and Adindani 1963; Bandel and Kuss 1987; Kuss et al. 2000). The thickness of this succession gradually decreases towards the south, confirming deposition during marine transgressions that came mainly from the north (Klitzsch 1990; Klitzsch et al. 1990; Kuss and Bachmann 1996; Kora 1998).

The NGP rises significantly above the lowland of Wadi Araba in the south and gently slopes towards Wadi Ghewibba in the north (Fig. 1b). In general, the Northern and Southern Galala plateaus are NE–SW oriented, representing a major branch of the Syrian Arc structure in the northern part of the Eastern Desert of Egypt (e.g., Said 1962). This arc consists of a belt of complex uplifts and domal anticlines that can be traced from Syria to the central part of the Western Desert of Egypt, passing through northern Sinai and the northern Eastern Desert (Fig. 1a) (Said 1962; Meshref 1990; Shahar 1994). Folding and/or uplift of the Syrian Arc were active during the Late Cretaceous (post-Cenomanian times) and extended into Early Palaeogene (Meshref 1990; Moustafa 2002, 2013; Höntzsch et al. 2011), associated with the closure of the Neo-Tethys Ocean (Lüning et al. 1998; Stampfli et al. 2001). Furthermore, upper Palaeozoic rocks of the eastern side of the NGP are folded and faulted against the Cretaceous–Eocene succession, forming several horsts and grabens (Fig. 1c) (e.g., Said 1962; Abdallah and Adindani 1963).

Material and methods

In the measured Carboniferous–Permian succession, stratigraphical, sedimentological and palaeontological data were gathered through detailed field descriptions of each bed. Sedimentary textures, sedimentary structures, nature of bedding and bedding contacts, faunal and/or floral content, and the lateral variability for each bed have been documented along an area of about 750 m to the northwest and to the southeast of Wadi Aheimer. A total of 123 rock samples have been collected from each characteristic facies. Ichnological field observations were concentrated on the identification of ichnogenera and document their distribution along the exposed succession. The size of the trace fossils and their physical interrelationships (e.g., interpenetrating, intercalated or isolated occurrences) were noted. Careful investigation has also been made to the ichnological aspects that allow the ichnofabric characterisation, such as trace fossil assemblage, tiering, cross-cutting relationships and the Ichnofabric Index. In addition, representative rock samples (27 samples) containing some of these trace fossils have been collected for detailed investigations. They were marked with arrows to indicate *in-situ* orientations within the bed and photographed.

In the laboratory, standard thin-sections of 57 rock samples were examined for their petrography. In addition, a total of 11 moderately to badly-preserved brachiopod specimens were treated with a dilute hydrogen peroxide solution to remove adhering matrix for identification. Furthermore, some moderately preserved plant remains in five rock samples were identified. All rock and fossil samples are housed

in the collections of the Department of Geology, Faculty of Science, Alexandria University. Numbers of rock samples are prefixed by WA for the Wadi Aheimer section.

Stratigraphy

Lithostratigraphy

Wadi Aheimer exposes the stratotype section of the upper Palaeozoic Aheimer Formation (Abdallah and Adindani 1963). This formation is exclusively recorded in outcrops from the NGP in the western side of the Gulf of Suez region (Tables 1, 2). In the study area, the Aheimer Formation is overlain unconformably either by the Permo–Triassic red beds of the Qiseib Formation or by the lower Cretaceous pebbly sandstones of the Malha Formation (Said 1962; Abdallah and Adindani 1963). Southward, the Aheimer Formation has been considered to overlie conformably or to interfinger with the Abu Darag Formation (Awad and Said 1966; Klitzsch 1990) or with the Rod El Hamal Formation (Said 1971). In fact, these three formations are characterised by unexposed bases. Therefore, the exact superposition of these formations is uncertain.

The Aheimer Formation consists of sandstones and siltstones alternating with fossiliferous shale and dolomite beds, commonly in repetitive cycles (Figs. 2, 3). It attains a thickness of about 250 m. Noteworthy is the great change in thickness of this formation from place to place within short distances. The studied succession is herein subdivided into four informal rock units, from oldest: unit I, II, III and IV (Figs. 3, 4a). These units are correlated with some lithostratigraphic schemes that have been proposed to describe the upper Palaeozoic deposits in the eastern side of the NGP (Table 2).

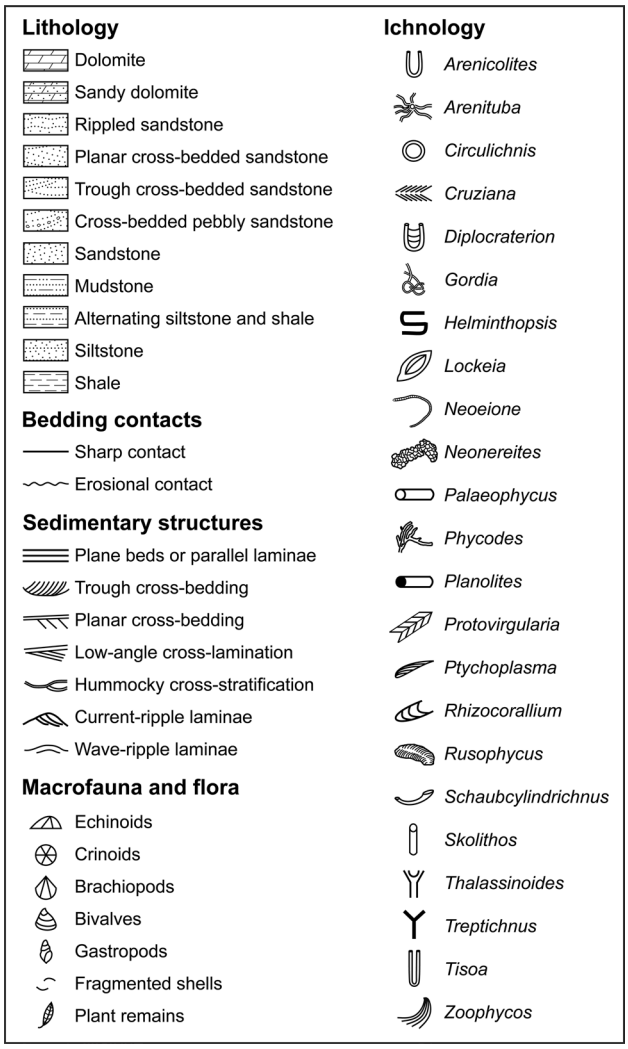

Fig. 2 Legend of symbols used for sedimentological and ichnological structures and macrofossils

Table 2 Correlation of rock units of the Aheimer Formation recognized in the measured type section with those defined in some selected previous studies

Abdallah and Adindani (1963)	Abd El-Azeam (1990)	Kora and Mansour (1992)	El-Barkooky (1994)	Present work
Transitional strata	Unit IV (early Permian)		Sequence IV (early–late Permian)	
3- The upper unit: sandstone, shale and silts (early Permian)	Unit III (early Permian)	Upper member (early Permian)	Sequence III (early–late Permian)	Unit IV (early Permian)
2- The middle unit: limestone-sandstone (early Permian)	Unit II (early Permian) Unit I (late Carboniferous)	Middle member (early Permian)	Sequence II (early Permian)	Unit III (early Permian) Unit II (early Permian)
1- The lower unit: *Lophophyllidium*-bearing shale series (late Carbo.)		Lower member (late Carboniferous)	Sequence I (late Carboniferous)	Unit I (the *Tisoa*-bearing unit) (late Carboniferous)

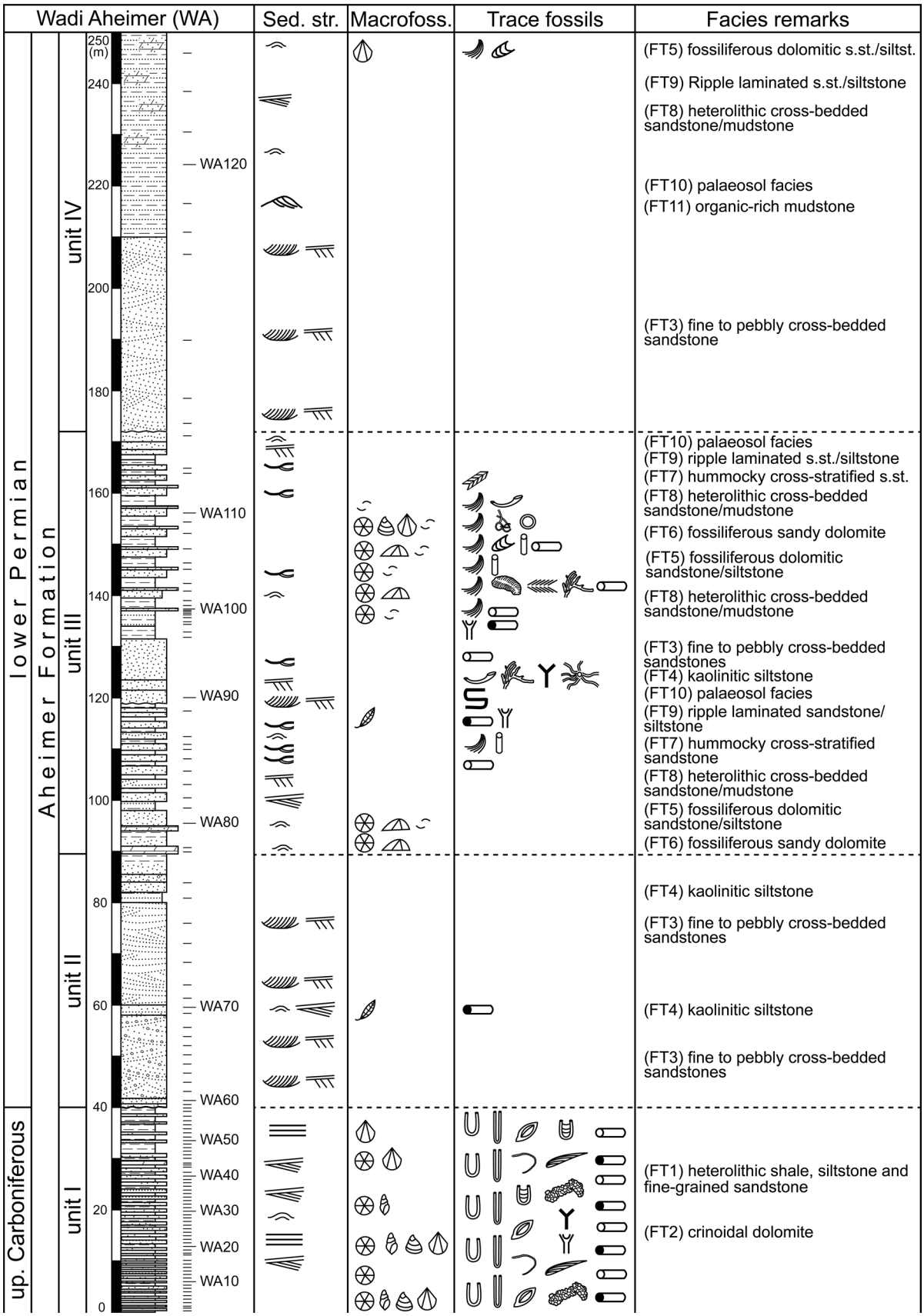
Wadi Aheimer (WA)
Sed. str.
Macrofoss.
Trace fossils
Facies remarks
lower Permian
Aheimer Formation
up. Carboniferous
unit IV
unit III
unit II
unit I
250 (m)
240
220
200
180
160
140
120
100
80
60
40
20
0
WA120
WA110
WA100
WA90
WA80
WA70
WA60
WA50
WA40
WA30
WA20
WA10
(FT5) fossiliferous dolomitic s.st./siltst.
(FT9) Ripple laminated s.st./siltstone
(FT8) heterolithic cross-bedded sandstone/mudstone
(FT10) palaeosol facies
(FT11) organic-rich mudstone
(FT3) fine to pebbly cross-bedded sandstone
(FT10) palaeosol facies
(FT9) ripple laminated s.st./siltstone
(FT7) hummocky cross-stratified s.st.
(FT8) heterolithic cross-bedded sandstone/mudstone
(FT6) fossiliferous sandy dolomite
(FT5) fossiliferous dolomitic sandstone/siltstone
(FT8) heterolithic cross-bedded sandstone/mudstone
(FT3) fine to pebbly cross-bedded sandstones
(FT4) kaolinitic siltstone
(FT10) palaeosol facies
(FT9) ripple laminated sandstone/ siltstone
(FT7) hummocky cross-stratified sandstone
(FT8) heterolithic cross-bedded sandstone/mudstone
(FT5) fossiliferous dolomitic sandstone/siltstone
(FT6) fossiliferous sandy dolomite
(FT4) kaolinitic siltstone
(FT3) fine to pebbly cross-bedded sandstones
(FT4) kaolinitic siltstone
(FT3) fine to pebbly cross-bedded sandstones
(FT1) heterolithic shale, siltstone and fine-grained sandstone
(FT2) crinoidal dolomite

◂**Fig. 3** Composite lithological log and sedimentary structures (Sed. str.), macro- and trace fossils, and facies distribution of the upper Carboniferous−lower Permian Aheimer Formation. For a key to symbols used see Fig. 2

Unit I

This unit consists of intercalated shale, clayey and/or dolomitic siltstone, sandstone and sandy dolomite (Figs. 3, 4b). It represents the oldest unit exposed in the study area, attaining a thickness of about 40 m. Southward, near Bir Abu Darag, it reaches a thickness of about 60 m (e.g., Abdallah and Adindani 1963). The basal 32 m of this unit is composed of dark grey shale (organic-rich in parts), intercalated with reddish brown ferruginous hard siltstone, sandstone and sandy dolomite interbeds (Fig. 4b). The thickness of each bed ranges from about 0.1 to 0.5 m, increasing upward, with sharp contacts. Up-section (between 32 and 40 m), variegated fissile shale dominates, alternating with laminated, wave-rippled, thin-bedded siltstones and fine-grained sandstones (Figs. 3, 4c).

Unit I is the richest fossil-bearing horizon encountered in the study area. Sediments are highly burrowed (Fig. 3), represented by simple vertical and deep burrows (see 'Ichnological analysis' below). In addition, poorly-preserved crinoid columnals, bivalves, small gastropods, brachiopods (*Antiquatonia* sp., *Rhynchopora* sp.; Fig. 4h, j) and bryozoans occur (Fig. 3). Furthermore, intervals enriched in microfauna are also recorded. Agglutinated foraminifera are the most common microfaunal element, followed by microgranular forms. Ostracod and conodont elements, in contrast, play only a minor role. Based on different macro- and microfossil assemblages, several studies support a Late Pennsylvanian (Westphalian−Stephanian) age for this unit (Omara and Vangerow 1965; Said and Eissa 1969; Herbig and Kuss 1988; Klitzsch 1990; Kora 1998; present study). Unit I is correlated with the lower *Lophophyllidium*-bearing shale of Abdallah and Adindani (1963), the lower part of unit I of Abd El-Azeam (1990), the lower member of Kora and Mansour (1992) and sequence I of El-Barkooky (1994) (Table 2).

It is worthy of mention that the lower *Lophophyllidium*-bearing shale unit was introduced by Abdallah and Adindani (1963) in an area about 8 km to the SW of the Wadi Aheimer succession based on the apparently abundant horn coral *Lophophyllidium*. However, our field observations of this unit at the area west of the Gulf of Suez in the Wadi Aheimer and Abu Darag areas (for about 30 km SE of the Wadi Aheimer succession) reveal that the occurrence of this rugose coral is remarkably scarce. Therefore, the pertinence of this nomenclature is debatable. Instead, the characteristic feature throughout this unit is the high abundance of elongate vertical burrows of the *Tisoa* ichnotaxon (see 'Ichnological analysis' below). Therefore, we inclined to designate this unit as "the *Tisoa*-bearing unit" to characterise the latest Carboniferous sediments and mark the Carboniferous/Permian boundary particularly in the study type section of the Aheimer Formation.

Unit II

Unit II (about 50 m thick) is dominated by cross-bedded sandstones and siltstones, unconformably overlying unit I (Figs. 3, 4c). The base of this unit is characterised by a lens of massive sandstone (about 0.5 m thick) and underlies a thin light grey hard laminated kaolinitic siltstone layer (about 1.0 m thick). Above (41.5−58 m) is yellow, thick, moderately cemented, tabular and trough cross-bedded pebbly sandstone (Fig. 4c), containing clasts up to 7 cm long near the base. Pebbles vary in size laterally and are mostly composed of mono- and polycrystalline quartz. In addition, the amount of pebbles gradually decreases in the upper part of this unit. Between 58 and 60 m, sandstone sediments become finer and grade to siltstone with plant remains (Fig. 4d). This siltstone layer is followed by a reddish yellow, moderately cemented, tabular and trough cross-bedded, medium- to fine-grained sandstone bed (60−80 m). The uppermost part of unit II (80−90 m) consists of sandstone, siltstone and shale interbeds (Fig. 3).

Noteworthy is the complete absence of marine macro- and microfossils in unit II. However, some plant remains (*Calamites* sp.) and rare trace fossils are recorded (Figs. 3, 4d). *Calamites* lived during the Carboniferous and Permian periods (e.g., Rafferty 2011). Based on the sharp stratigraphic discontinuity with the underlying unit I (Figs. 3, 4c; see 'Sequence stratigraphy' below), an Early Permian age could be suggested to unit II. This unit is correlated with the lower part of the middle limestone-sandstone of Abdallah and Adindani (1963), the upper part of unit I of Abd El-Azeam (1990), the lower part of the middle member of Kora and Mansour (1992) and the lower part of sequence II of El-Barkooky (1994) (Table 2).

Unit III

This unit attains a thickness of about 82 m (interval between 90 and 172 m; Fig. 3), and consists of yellowish white to reddish sandstone, light grey to white partly kaolinitic siltstone and variegated shale interbeds (Figs. 3, 4e). This succession is intercalated with two to three thin brownish ferruginous hard highly fractured and fossiliferous sandy dolomite beds that increase in number near the top of the unit (up to seven ledges; Fig. 4l). Sandstone layers are partly rippled laminated (Fig. 4e), fractured, hummocky cross-bedded, fine- to medium-grained, highly burrowed and dolomitic in parts (Fig. 3). The thickness of

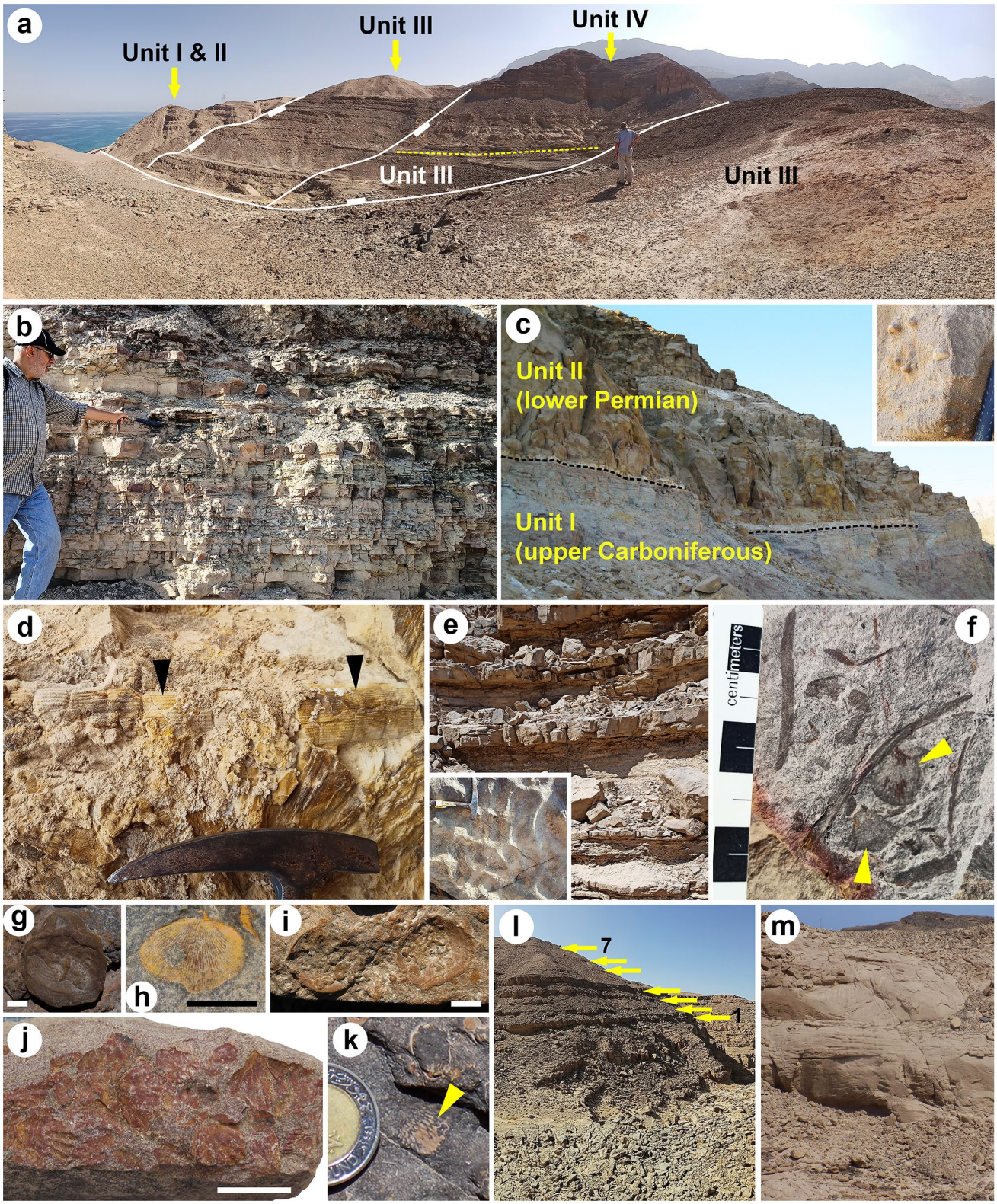

some beds in this unit varies greatly. Some ferruginous truncation surfaces also occur, representing erosive or omission surfaces that can be traced laterally.

Shale layers in the lower part of unit III, between 115 and 119 m, contain some plant remains (Figs. 3, 4f). The identified samples include *Ginkgo*-like fossil leaves that can be traced back to the Early Permian (e.g., Florin 1949). In

◂**Fig. 4** Some field aspects of the studied section. **a** At Wadi Aheimer, the upper Carboniferous−lower Permian succession is subdivided into four stratigraphic units (I−IV). Note the effect of faulting on these units. **b** Unit I is characterised by organic-rich shale, siltstone and sandstone with sandy dolomite interbeds. **c** The upper Carboniferous unit I is unconformably capped by the lower Permian unit II. Pebbly sandstone (inset) is common in the basal part of unit II. **d** *Calamites* sp. (arrows) in the lower part of unit II (at 58−60 m in Fig. 3). **e** Rippled sandstone (inset), siltstone and shale interbeds in unit III (at 110−118 m in Fig. 3). **f** The *Ginkgo*-like fossil leaves (arrows) in unit III (at 110−118 m in Fig. 3). **g** *Linoproductus* sp., unit III. **h** *Antiquatonia* sp., unit I. **i** *Rhipidomella* sp., unit III. **j** Cluster of *Rhynchopora* sp., unit I. **k** Part of a sheet-like bryozoan colony (arrow), unit III. **l** Seven dolomite ledges (1−7) occur in the upper part of unit III, between 135 and 165 m in Fig. 3. **m** Cross-bedded bulging sandstone in unit IV of the studied Wadi Aheimer succession (at 172−210 m in Fig. 3). Scale bars = 1.0 cm

addition, dolomite layers are fossiliferous with some thin-shelled brachiopods (e.g., *Composita* sp., *Dielasma* sp., *Linoproductus* sp., *Rhipidomella* sp.; Fig. 4g, i), crinoid fragments, bryozoans (Fig. 4k) and fusulinid foraminifer, confirming likewise an Early Permian age (cf. Kora and Mansour 1992; Kora 1998). Furthermore, sandstone beds are highly burrowed with abundant trace fossils (Fig. 3; see 'Ichnological analysis' below). This unit is correlated with the upper part of the middle limestone-sandstone of Abdallah and Adindani (1963), unit II of Abd El-Azeam (1990), the upper part of the middle member of Kora and Mansour (1992) and the upper part of sequence II of El-Barkooky (1994) (Table 2).

Unit IV

This unit is mainly composed of sandstone, siltstone and shale, attaining a thickness of about 78 m (interval between 172 and 250 m; Fig. 3). The lower part of this unit (172−210 m) consists of yellowish, fine- to medium-grained, planar to trough cross-bedded sandstones (Fig. 3), having remarkable bulging steep slopes (Fig. 4m) and laterally extending throughout the study area. The upper part (interval between 210 and 250 m) consists of shales, cross-bedded sandstones, and siltstones. In addition, some dolomitic sandstone lenses are sporadically recorded (Fig. 3). The basal dark grey shale (210−218 m) overlies the lower bulging sand body (Fig. 3) and is non-fossiliferous, organic rich and gypsiferous. Above are very thin interbeds of red siltstone and very fine sandstone. The upper part of shale (about 32 m thick) is sandier and exhibits ripples and lenticular bedding. In the topmost part of unit IV, sandstone sediments yield rare brachiopod imprints and trace fossils (Fig. 3).

In Wadi Araba, about 60 km to the south of the study area, Lejal-Nicol (1990) described a typical Permian flora from deposits of the upper member of the Aheimer Formation. In addition, early Permian fossil algae have been recorded from these sediments (Omran and Khalifa 1988). Furthermore, overlying the Aheimer Formation, the lower multi-coloured clastic part of the Qiseib Formation (Abdallab and Adindani 1963) contains fossil tree trunks and other plant remains, documenting an Early Permian age (see Klitzsch 1990). In view of the rare occurrence of trace and macrofossils and based on the stratigraphic continuity with the underlying unit III, an Early Permian age could be extrapolated to include also unit IV of the studied Aheimer Formation. This unit is correlated with the upper sandstone, shale and silts of Abdallah and Adindani (1963), unit III of Abd El-Azeam (1990), the upper member of Kora and Mansour (1992) and sequence III of El-Barkooky (1994) (Table 2).

Sequence stratigraphy

Three well defined unconformities have been recognized within the study succession. These surfaces define four 3rd-order depositional sequences that are named according to the area of definition (depositional sequence Northern Galala, DS NG 1−4; Fig. 5). The sequence-stratigraphic stacking patterns of facies, key surfaces and systems tracts have been recognized by several criteria based on the works of Ernst et al. (1996), Coe (2003), Embry (2009), Catuneanu et al. (2011) and Catuneanu (2017, 2019).

Depositional sequence NG 1

DS NG 1 is of Late Carboniferous age and comprises the complete unit I (the *Tisoa*-bearing unit) of the Aheimer Formation (Fig. 5a). Deposits consist of repetitive cycles of highly burrowed shale, siltstone, sandstone, and sandy dolomite interbeds, confirming the occurrence of an aggrading shelf (Van Wagoner et al. 1990) that is characterised by a shallowing and coarsening-upward vertical stacking pattern of facies (Figs. 5a, b, 6a). The recorded aggradational parasequence sets that are truncated by a sequence boundary document the occurrence of an early highstand systems tract (HST) (Catuneanu 2006). In view of the exposure, only the HST of this sequence is present (Fig. 5a). The sequence boundary capping DS NG 1, SB1, is described in the next section.

Depositional sequence NG 2

DS NG 2 comprises the basal lower Permian sediments of the studied succession. It includes the entire unit II and the lower part of unit III (Fig. 5a), attaining a thickness of about 80 m. The lower part of this sequence consists of cross-bedded pebbly sandstones and kaolinitic siltstone and is followed by mudstone and sandstone with fossiliferous dolomite interbeds (Fig. 5a, b). The basal sequence boundary of DS NG 2, SB1, is represented by the erosional

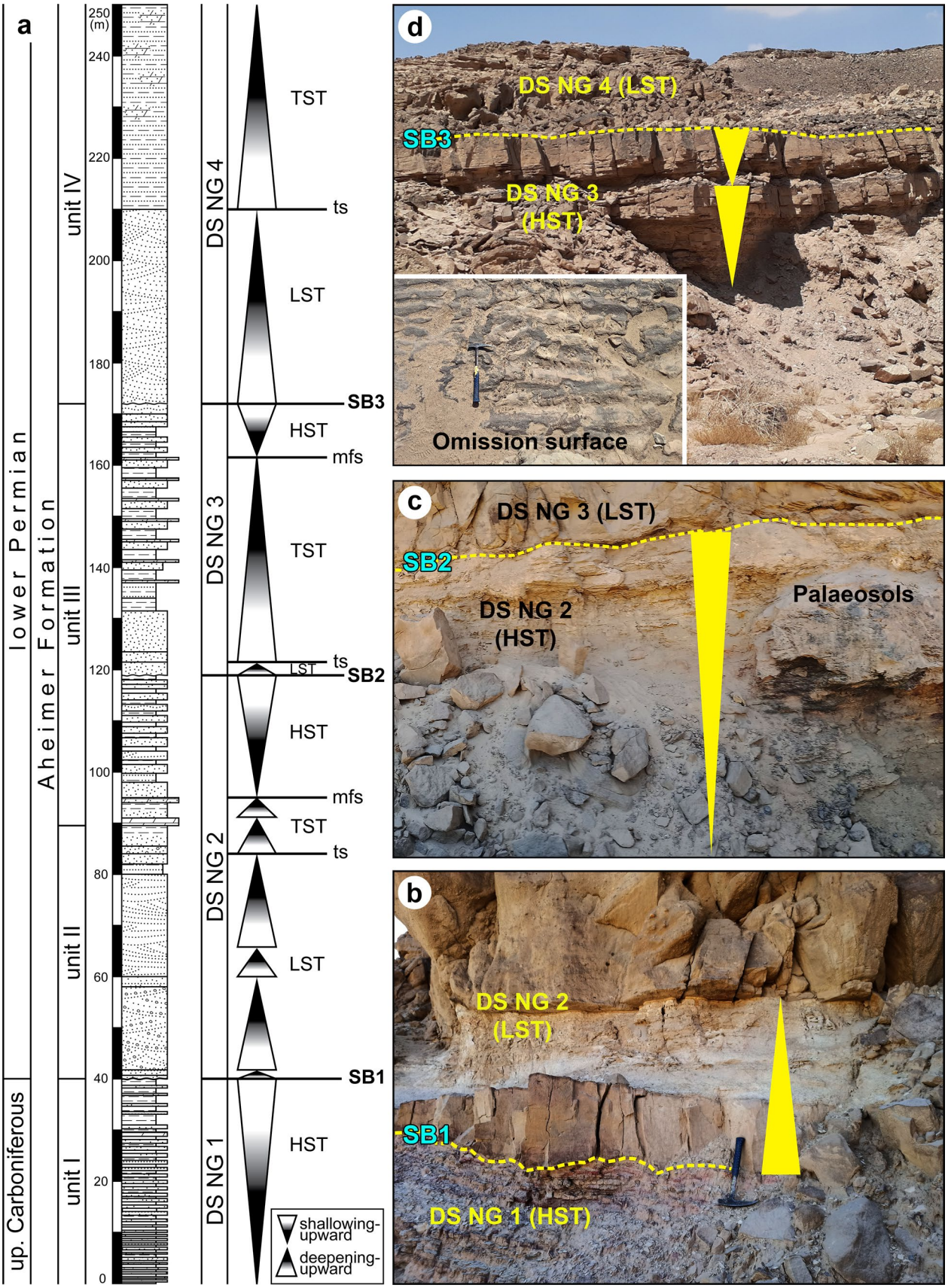
a
lower Permian
Aheimer Formation
up. Carboniferous
unit I
unit II
unit III
unit IV
250 (m)
240
220
200
180
160
140
120
100
80
60
40
20
0
DS NG 4
DS NG 3
DS NG 2
DS NG 1
TST
ts
LST
SB3
HST
mfs
TST
ts
LST
SB2
HST
mfs
TST
ts
LST
SB1
HST
shallowing-upward
deepening-upward
d
DS NG 4 (LST)
SB3
DS NG 3 (HST)
Omission surface
c
DS NG 3 (LST)
SB2
DS NG 2 (HST)
Palaeosols
b
DS NG 2 (LST)
SB1
DS NG 1 (HST)

◂**Fig. 5** Sequence-stratigraphical interpretation of the Aheimer Formation and photos of the outcrop. **a** Stratigraphical log of the Wadi Aheimer section with sequence stratigraphic interpretation. **b** The first sequence boundary (SB1) between DS NG 1 and 2. Note the change from the aggradational stacking pattern of deposits of the HST in DS NG 1 to the LST fluvial facies in the basal part of DS NG 2. Arrow marks the first fining-upward cycle overlying the SB1. **c** The second sequence boundary (SB2) between the HST of DS NG 2 and the LST of DS NG 3. Arrow marks the coarsening-upward cycle underlying the SB2. Palaeosol characterises the topmost part of the HST of DS NG 2. **d** The coarsening-upward cycles in the HST of DS NG 3. Note the omission surface (inset) characterising the third sequence boundary (SB3)

contact of pebbly and coarse-grained sandstone strata atop the aggradational parasequences sets of DS NG 1 (Fig. 5b). The following lowstand systems tract (LST) consists of fluvial multi-storey channel facies associated with four fining-upward units of a high to low energy fluvial system (Figs. 5a, b, 6b). These sediments are considered as an incised valley fill based on its erosional base and rapid lateral thickness changes (Catuneanu et al. 2011). Quartz pebbles in the lower part of this LST may indicate transport within the flooded valley. The transgressive systems tract (TST) starts with a thin lag deposit of pebbly sandstone, representing a transgressive ravinement surface (Nummedal and Swift 1987) that is defined as an erosional surface resulting from wave scouring (i.e., wave ravinement surfaces) (Swift 1975) or tidal scouring (tidal ravinement surface) (Allen and Posamentier 1993) during transgression (Fig. 6c). This ts surface is followed by a retrogradational stacking pattern of deepening-upward cycles of marine facies (Figs. 5a, 6c). The highly fossiliferous dolomite layer characterises the maximum flooding surface (mfs) that is also confirmed by the occurrence of fining-upward cycles below and coarsening-upward cycles above (Fig. 6c). The HST consists of five coarsening-upward cycles of mudstone and sandstone interbeds (Fig. 6d).

Depositional sequence NG 3

DS NG 3 is represented by the upper part of unit III of the Aheimer Formation (about 50 m thick; Fig. 5a). It consists of sandstone, shale, mudstone, fossiliferous dolomitic sandstone and fossiliferous sandy dolomite interbeds. The basal sequence boundary SB2 is marked by karstification, palaeosols and extensive omission surface (Fig. 5c). Along this surface, marine strata of the topmost part of DS NG 2 are truncated by a thin (2−3 m thick) fining-upward cycle of unfossiliferous sandstone and mudstone of fluvial origin, representing part of the LST (Figs. 5c, 6e). In contrast to the first sequence boundary (SB1), SB2 is almost flat with low relief and non-conglomeratic (Fig. 5c), supporting the absence of an incised valley here.

The following TST is characterised by seven fining-upward marine cycles of highly burrowed and fossiliferous dolomitic sandstone, fossiliferous sandy dolomite and shale (Fig. 5a) deposited mostly in shoreface environments. Thus, the surface between the LST and TST represents a marine flooding surface (i.e., ts), recording a deepening event. It may be considered as a transgressive ravinement surface (cf. Nummedal and Swift 1987). Laterally, the transgressive surface (ts) of DS NG 3 is amalgamated with SB2 due to the lack of accommodation space during deposition of the LST (Fig. 6f). The lower part of this TST is characterised by the predominance of siliciclastic facies whereas carbonate deposits become increasingly common in the upper part (Fig. 5a).

The mfs of DS NG 3 is represented by the seventh dolomite layer (Fig. 5a). Based on the presence of an open-marine macrofauna and trace fossils, this carbonate layer represents the deepest part of this sequence and indicates the maximum transgression of the shoreline. This layer can clearly be distinguished and easily correlated across the study area. The HST consists of four cycles of fossiliferous sandy dolomite and heterolithic cross-bedded sandstone/mudstone facies that are followed by hummocky cross-stratified sandstone facies and ripple laminated sandstone/siltstone facies, confirming a shallowing-upward trend towards the end of the HST (Fig. 5a, d).

Depositional sequence NG 4

This depositional sequence attains a thickness of about 78 m, and comprises the entire unit IV (Fig. 5a). The recorded HST of DS NG 3 is truncated by the fluvial sandstone of DS NG 4, forming an extensive omission surface and representing the third sequence boundary (SB3) (Fig. 5d). The lower part of this sequence consists mainly of tabular and trough cross-bedded sandstones that are composed of clean sands (Figs. 4h, 5a). The stacking pattern of facies in this interval shows a fining-upward of the LST that resulted from braided streams (Fig. 6g). This stacking pattern of facies containing the highest energy fluvial systems is comparable to the lowstand topset of a downstream-controlled sequence (Catuneanu et al. 2011; Catuneanu 2019). The LST deposits are overlain by gypsiferous and organic-rich shale and red siltstone interbeds (about 8 m thick), representing deposition in restricted estuarine conditions. Therefore, the base of these estuarine facies is selected to define the transgressive surface (ts) of this sequence (Figs. 5a, 6g).

The upper part of this sequence consists of shale, siltstone and sandstone interbeds and is characterised by flat and rippled lamination, ripples and lenticular bedding. The stacking pattern of facies in this part shows an aggrading to a retrograding pattern, which might be the result of a general

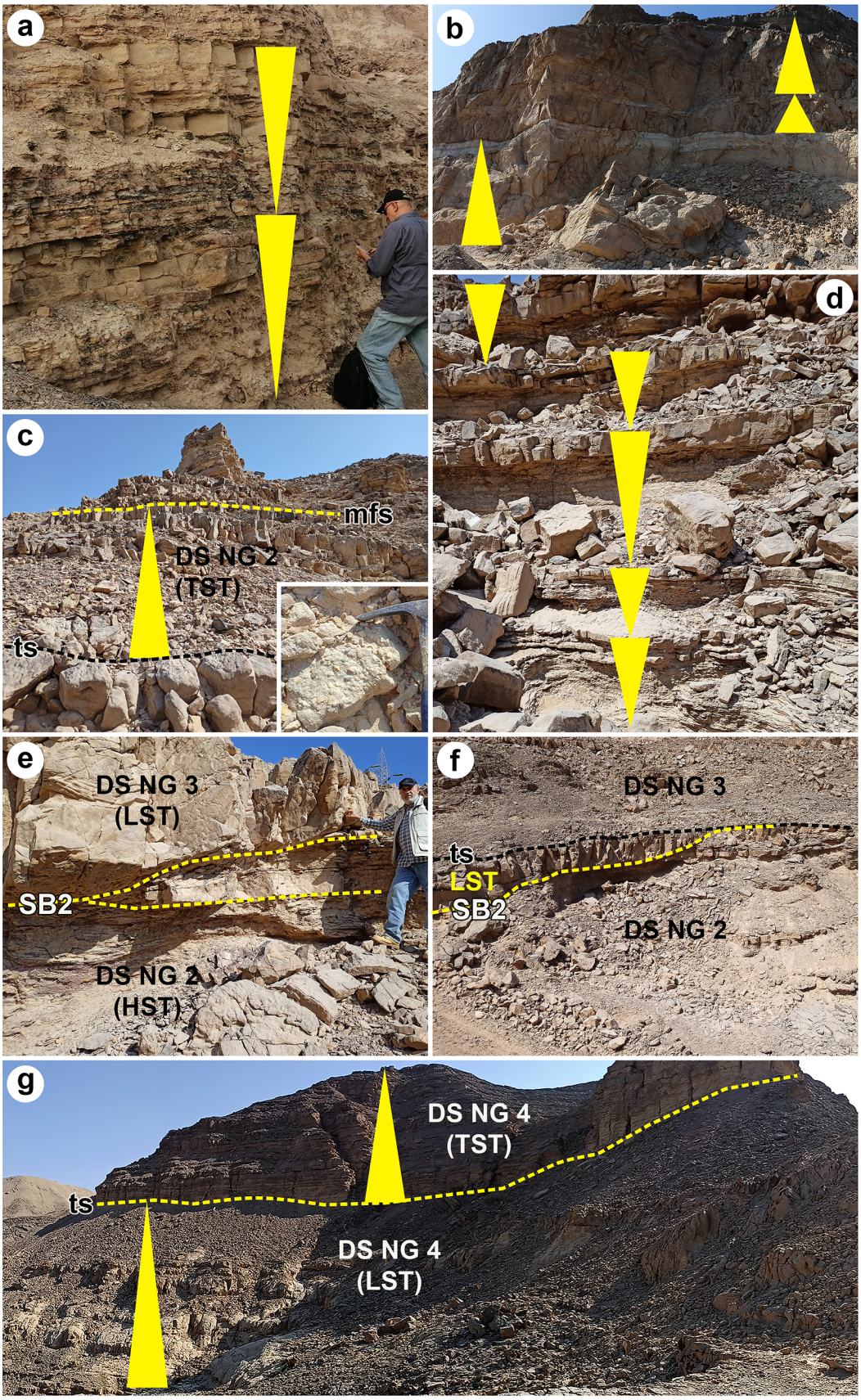
a
b
c
mfs
DS NG 2
(TST)
ts
d
e
DS NG 3
(LST)
SB2
DS NG 2
(HST)
f
DS NG 3
ts
LST
SB2
DS NG 2
g
DS NG 4
(TST)
ts
DS NG 4
(LST)

◂**Fig. 6** Sequence-stratigraphical framework of the section studied. **a** Coarsening-upward cycles in an aggradational stacking pattern of the HST in DS NG 1. **b** Part of the lowstand systems tract of DS NG 2 with the upper three fining-upward cycles. **c** The transgressive surface (ts), maximum flooding surface (mfs) and transgressive systems tract (TST) of DS NG 2. Note the fining-upward cycle characterising the TST and the occurrence of a pebbly sandstone layer (inset) coinciding with the recorded ts. **d** Sandstone, siltstone and shale interbeds in the HST of DS NG 2. Note the coarsening-upward cycles characterising this systems tract. **e** The truncation surface marks the second sequence boundary (SB2) between the HST and LST of DS NG 2 and 3, respectively. **f** Truncation of DS NG 2 by fluvial sediments of the LST of DS NG 3. Note that the transgressive surface (ts) is laterally amalgamated with the second sequence boundary (SB2). **g** Panoramic view of DS NG 4 showing the transgressive surface (ts) between the LST and TST. Both systems tracts show fining-upward cycles

transgressive phase. These TST facies mostly reflect upper to middle shoreface depositional settings.

Regionally, the four recorded upper Carboniferous−lower Permian sequences in the studied section are considered as a part of the first-order mega-sequence of the Arabian plate (AP5) of Sharland et al. (2001). The lower boundary of this AP5 sequence is marked by the 'Hercynian unconformity' or the 'pre-Unayzah unconformity' (Sharland et al. 2001). The recorded sequences can also be correlated with the late Carboniferous second-order sequence of the Algerian Saharan Platform (Fekirine and Abdallah 1998), and with the upper part of the Carboniferous (NA4) and the lower part of the Permian (NA5) second-order sequence of North Africa (Carr 2002). The sequence boundary (SB5) between NA4 and NA5 represents the Carboniferous/Permian Hercynian Unconformity (Carr 2002).

Microfacies analysis

Microfacies analysis of the upper Carboniferous–lower Permian Aheimer Formation is based on investigation of rock thin-sections, supplemented by field observations of some features such as lithology, bedding, sedimentary structures and trace and body fossil content. Detailed petrographic analysis of the studied upper Palaeozoic succession has revealed a predominance of siliciclastic, with few carbonate (mainly dolomite) facies (Table 3). In siliciclastic facies, bioclasts are rare or nearly absent. In contrast, bioclasts are common in carbonate facies and are represented by crinoids, echinoids, brachiopods, bryozoans, benthic foraminifera and algae (Table 3; Figs. 7, 8, 9).

Facies analysis reveals 11 (micro-) facies types (FT1–FT11). All these facies types (nine siliciclastic and two carbonate) are described and interpreted. Based on similar attributes, the recorded 11 facies types are grouped into four different facies associations (FA1–FA4), representing a wide spectrum of depositional environments. They include: (FA1) intertidal to shallow subtidal facies association, (FA2) fluvial channel fill/overbank facies association, (FA3) upper shoreface to offshore transition facies association, and (FA4) interdistributary bay and/or restricted estuarine facies association (Table 3).

Ichnological analysis

Trace fossil assemblages

Trace fossils occur throughout the studied stratigraphic succession. They are highly abundant in units I and III (Fig. 3). The recorded ichnofossil assemblages are composed of horizontal, vertical, and sub-vertical traces attributable to the activity of a variety of crustaceans, polychaetes, bivalves and arthropods. At least 26 ichnotaxa, belonging to 23 ichnogenera, have been identified (Table 4; Figs. 10, 11, 12, 13). Stratigraphically, nine ichnotaxa (34.6%) were exclusively reported from the upper Carboniferous sediments (i.e., unit I), 12 (46.2%) from the lower Permian unit III, two (7.7%) from the lower Permian unit III and IV, two (7.7%) from unit I and III (i.e., upper Carboniferous−lower Permian), whereas a single ichnotaxon (3.8%) was reported from the upper Carboniferous−lower Permian sediments of unit I, II and III. These traces belong to five ethological categories, including domichnia, fodinichnia, cubichnia, pascichnia and repichnion (Table 4).

The mud-dominated sediments of unit I are highly burrowed. Burrows recorded include vertical and sub-vertical dwelling structures of inferred suspension-feeding organisms (e.g., *Arenicolites* isp., *Diplocraterion parallelum*, *Thalassinoides suevicus*, *Tisoa siphonalis*) and deposit feeders such as *Neoeione moniliformis*, *Neonereites multiserialis*, *Palaeophycus* isp., *Planolites* isp., *Th. suevicus* and *Treptichnus* isp. (Table 4; Figs. 10, 11, 12, 13). Some horizontal traces, including *Lockeia siliquaria*, *Lockeia* isp. and *Ptychoplasma* cf. *excelsum* are also recorded (Figs. 10e, h, i, 11a, g). Most of the abundant vertical and sub-vertical burrows are long and narrow with sharp to irregular walls, passively filled, and usually paired (Fig 12g−i, Fig. 13a−c). It is remarkable that the tops of the abundant U-burrows of *Tisoa* usually start from the upper surfaces of five siltstone layers recognised in unit I (Figs. 12i, 13b). These burrows may penetrate strata up to 1.5 m depth and thus they could be considered as the longest vertical burrows recorded in this study.

Up-section, a distinctly different ichnocoenosis is recorded within the sandstone-dominated intervals of unit II. It is represented by the monospecific occurrence of a low-density population of *Planolites* isp. (Fig. 3). In contrast to the underlying strata, unit III is dominated by a characteristic burrowing structure (Fig. 3). Based on the distribution of trace fossils, unit III can be subdivided into two parts. In the lower one (between 90 and

Table 3 Facies association (FA) and characteristic features of facies types (FT) in the studied section and their depositional setting

FA	FT and name	Occurrence	Components and remarks	Sedimentary structures	Depositional environment
FA1	FT1: Heterolithic shale, siltstone and fine-grained sandstone (Fig. 7a–c)	Unit I	Intercalation of medium to thin beds of reddish fine-grained sandstone, siltstone and variegated fissile shale, highly ferruginous, with microfossils and sporadic macrofossils	Flat bedding and lamination, low angle planar cross-lamination, symmetric wave ripple lamination, mud drapes, bioturbation with vertical and horizontal burrows	Shallow subtidal to intertidal (Richards 1994)
	FT2: Crinoidal dolomite (Fig. 7d)	Unit I	Brownish crinoid and echinoid fragments and spines embedded in a coarse crystalline dolomite matrix	Planar laminated and wavy-rippled thin beds	Shallow subtidal with some restriction (Tucker and Wright 1990; Flügel 2010)
FA2	FT3: Fine to pebbly cross-bedded sandstones (Fig. 7e, f)	Unit II, III, IV	Yellowish to reddish, moderately cemented, quartz arenitic, fine- to coarse-grained sandstone and pebbly sandstone	Trough and planar cross-bedding of varying scales with occasional ripple lamination	Low-sinuosity braided channel (Postma 1990; Miall 1996)
	FT4: Kaolinitic siltstone (Fig. 8a)	Unit II, III	Light grey kaolinitic siltstone to mudstone	Parallel and rippled lamination with low angles cross-lamination	Flood plain with inactive period of alluvial system (Kämpf and Schwertmann 1983; Miall 1996)
FA3	FT5: Fossiliferous dolomitic sandstone/siltstone (Fig. 8b, c)	Unit III, IV	Reddish to brownish, hard, ferruginous, quartz arenitic fine-grained sandstones and siltstones cemented by micro- to medium crystalline dolomite rhombs, different fine bioclasts	Planar laminated and wavy-rippled thin beds, bioturbation with vertical burrows	Lower to upper shoreface, (Clifton 2006)
	FT6: Fossiliferous sandy dolomite (Fig. 8d–f)	Unit III	Reddish to brownish, very hard, ferruginous, fine- to medium-crystalline fossiliferous dolomite with fine to coarse quartz grains embedded in a dolomite matrix, with fragments of crinoids, brachiopods, bryozoan, algae, and foraminiferal test	Planar laminated and wavy-rippled thin beds, bioturbation with vertical burrowing	Lower shoreface to offshore transition (Flügel 2010)
	FT7: Hummocky cross-stratified sandstone (Fig. 9a)	Unit III	Yellowish to brownish fine to medium-grained sandstones, quartz-arenitic type, ferruginous or clayey in parts	Hummocky cross-stratification	Lower to middle shoreface (Harms et al. 1982; Clifton 2006)
	FT8: Heterolithic cross-bedded sandstone/mudstone (Fig. 9b, c)	Unit III, IV	Yellowish to brownish, fine- to coarse-grained sandstone and mudstone, quartz arenitic type with calcareous and iron oxide cement, and fossiliferous in parts	Low angle planar and trough cross-bedding	Shoreface to offshore transition (Hunter et al. 1979; Galloway and Hobday 1996)
	FT9: Ripple laminated sandstone/siltstone (Fig. 9d, e)	Unit III, IV	Thin beds of fine to medium-grained, quartz arenitic sandstone with quartz overgrowth and iron oxide cements intercalated with clayey siltstone intervals. Some beds are typically mottled with the presence of black omission surfaces	Symmetrical rippled lamination grades, in part, to cross-lamination and cross-bedding, bioturbation	Middle to lower shoreface (Hunter et al. 1979; Galloway and Hobday 1996)

Table 3 (continued)

FA	FT and name	Occurrence	Components and remarks	Sedimentary structures	Depositional environment
FA4	FT10: Paleosol facies	Unit III, IV	Brownish to reddish, highly weathered, interbedded fine sand and mud sediments	Highly ferruginous indurated surface	Subaerial (Miall 1996)
	FT11: Organic-rich mudstone (Fig. 9f)	Unit IV	Dark grey gypsiferous mudstone and siltstone, intercalated with very fine to fine-grained sandstone	Massive to wavy laminated, with current ripples	Interdistributary bay and/or restricted estuary (Prothero and Schwab 1996)

132 m; Fig. 3), the ichno-assemblage comprises abundant *Arenituba* isp., *Palaeophycus* isp., *Planolites* isp., *Schaubcylindrichnus freyi*, *Skolithos* isp., *Treptichnus* isp., *Zoophycos* isp. and rare *Helminthopsis* isp. (Figs. 10, 11, 12, 13). This suite of trace fossils reflects the activity of organisms mainly with deposit-feeding and grazing behaviours (Table 4). In comparison to the lower part, the upper part of unit III (between 132 and 172 m; Fig. 3) is characterised by an abundant and diverse ichno-assemblage produced primarily by deposit-feeding organisms in addition to suspension feeders and grazers. It is composed of *Circulichnis* isp., *Cruziana* isp., *Gordia* aff. *marina*, *Palaeophycus* isp., *Phycodes* aff. *palmatus*, *Protovirgularia* isp., *Rhizocorallium* isp., *Rusophycus* cf. *carbonarius*, *Skolithos linearis*, *Thalassinoides paradoxicus* and *Zoophycos* isp. (Figs. 10, 11, 12, 13). In particular, *Zoophycos* appears to be the most common traces in this unit and occurs repeatedly at six different levels within the upper part of unit III (Figs. 3, 13d–f).

Apparently, the trace fossil assemblage of unit III changes laterally changed to a relatively moderate diversity in a section about 500 m to the southeast of the measured succession. It consists of the fodinichnia *Palaeophycus* isp., *Planolites* isp., *Rhizocorallum* isp., *Thalassinoides suevicus* and *Zoophycos* isp. (Table 4; Figs. 10, 11, 12, 13). On the other hand, the sandstone-dominated interval in the topmost part of unit IV is characterised by a rare occurrence of trace fossils. They are represented by traces produced primarily by deposit-feeding organisms, including *Rhizocorallum* isp. and *Zoophycos* isp. (Fig. 3).

In general, the aforementioned trace fossils of the Aheimer Formation are exceptionally diverse, abundant, and well preserved. In addition, due to invertebrate macrofossils, namely brachiopods, corals with fragmentary crinoid stems are uncommon and poorly-preserved in the Permo–Carboniferous strata of the Wadi Aheimer type section. Thus, the ichnological record of the Aheimer Formation is a significant contribution for more complete palaeoecological and palaeoenvironmental reconstructions of the study succession (see below).

Ichnofabric characterisation

According to trace fossil assemblage, tiering, cross-cutting relationships and Ichnofabric Index, the following ichnofabrics could be identified (Fig. 14).

Tisoa ichnofabric (Fig. 14a)

This ichnofabric occurs in the upper Carboniferous unit I (Fig. 3). It is characterised by dark grey shales, intercalated with reddish brown ferruginous hard siltstone, sandstone and sandy dolomite interbeds. Five colonization surfaces have

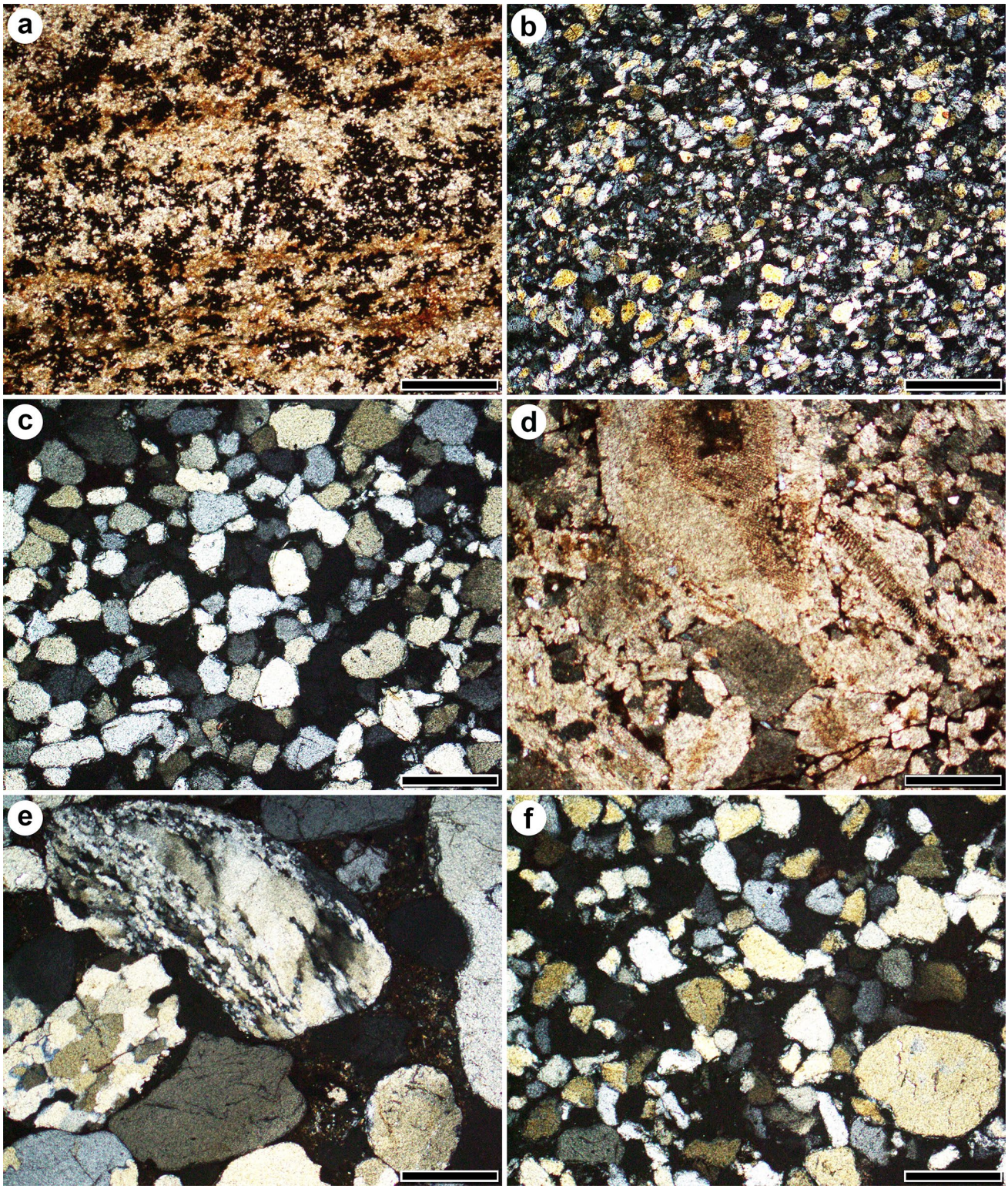

Fig. 7 Facies types (FT1−FT3). **a**−**c** FT1, heterolithic shale, siltstone and fine-grained sandstone. **a** Highly ferruginous laminated shale, WA42. **b** Siltstone dominated by silt-sized quartz grains and iron oxide cement, WA36. **c** Siliceous quartz arenitic sandstone, moderately to well-sorted, closely-packed grains, with silica overgrowths, WA17. **d** FT2, crinoidal dolomite showing longitudinal section and axial canal of crinoid fragments embedded in coarse crystals of dolomite rhombs with dark inclusions of iron oxide. Note the single crystal extinction for the crinoid fragment, WA44. **e**, **f** FT3, fine to pebbly cross-bedded sandstone. **e** Silicious quartz arenite with mono- and polycrystalline grains, WA61. **f** Siliceous quartz arenite showing fine, angular to subangular, closely-packed grains with pebbles and iron oxide cement, WA66. All photographs cross-polarized light (XPL), except for **a**, which plane polarized light (PPL). Scale bars = 0.5 mm

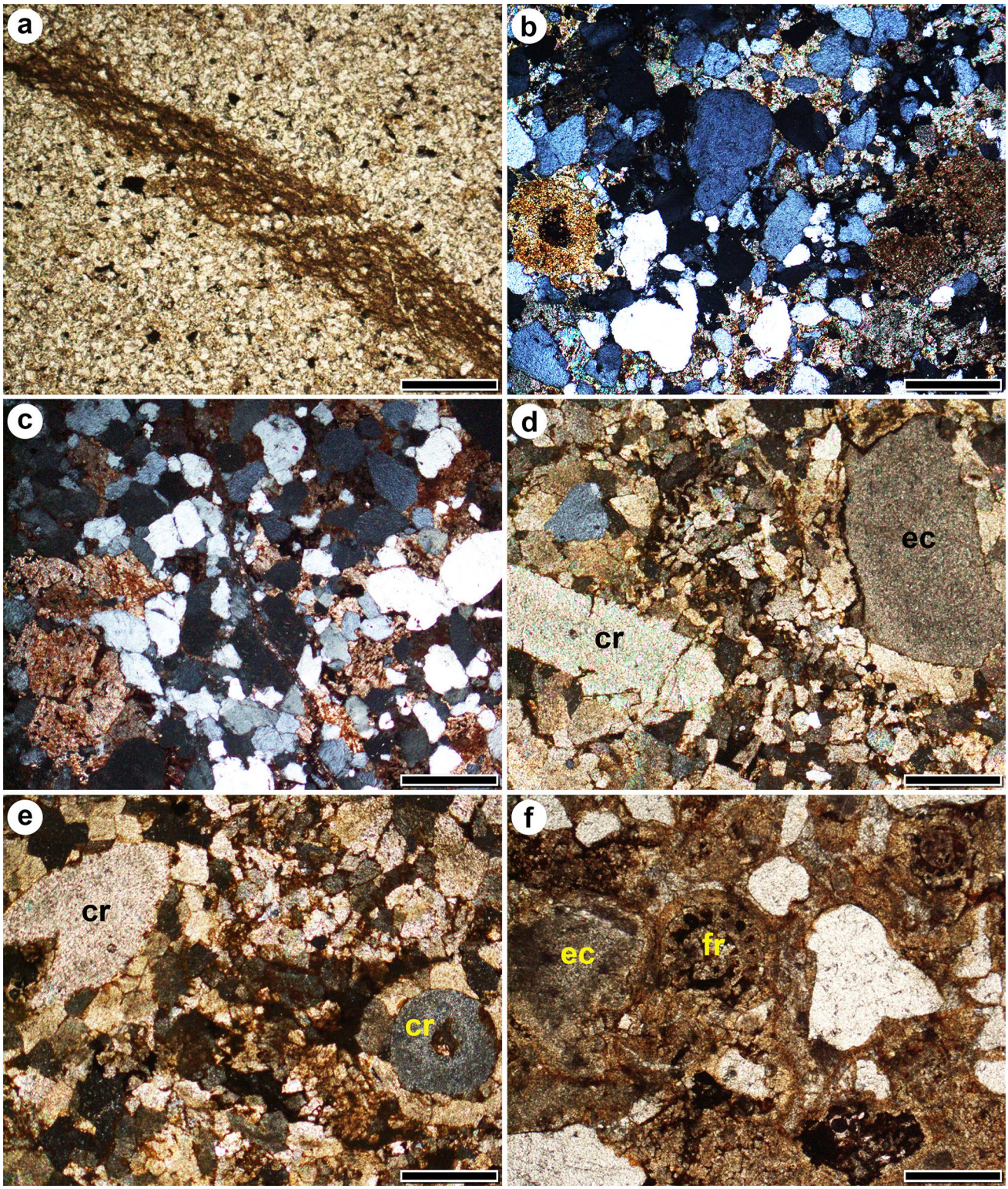

Fig. 8 Facies types (FT4−FT6). **a** FT4, kaolinitic siltstone dominated by silt-sized quartz grains and some iron oxide grains with layers of kaolinitic clay, WA69. **b**, **c** FT5, fossiliferous dolomitic sandstone/siltstone with some bioclasts embedded in a very fine to medium-grained, subangular to subrounded, closely-packed quartz arenite cemented by brownish micro- to coarse crystals of dolomite, WA105. **d**−**f** FT6, fossiliferous sandy dolomite showing some bioclasts as longitudinal and axial sections of crinoid fragments with single crystal extinction (cr), echinoids (ec), and fusulinid foraminifera (fr) embedded in coarse crystals of dolomite rhombs with dark inclusions of iron oxide. Fine to coarse quartz grains are also found, WA78, 78 and 79, respectively. All photographs XPL, except for **a** and **f**, which PPL. Scale bars = 0.5 mm

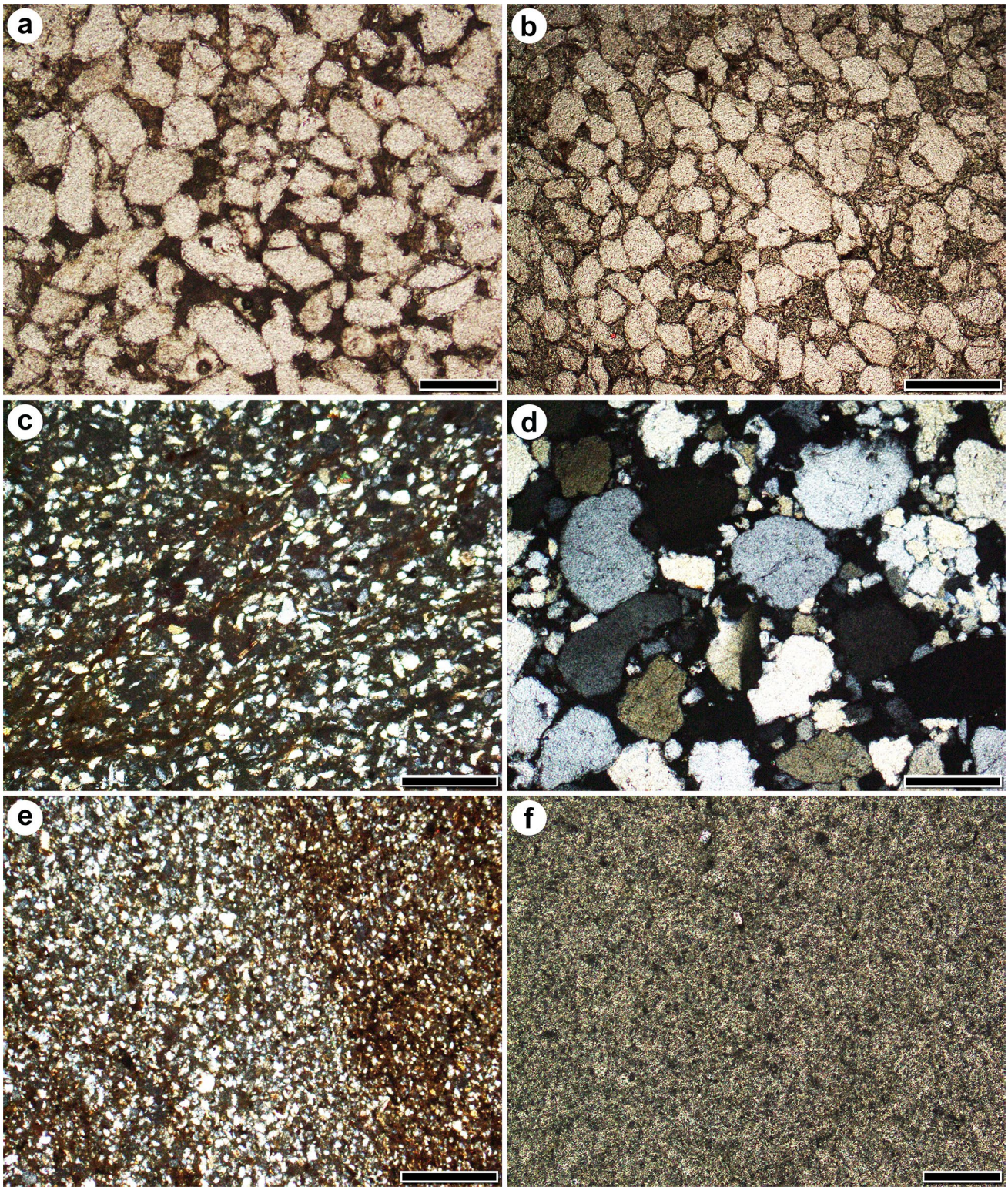

been recognized, indicating discontinuity surfaces, from which the abundant simple, vertical, U-shaped burrows of *Tisoa* penetrate the underlying strata. It has a sharply defined burrow margin and passive fill. The thin beds are extensively burrowed with an ichnofabric index (sensu Droser and Bottjer 1986) of 3 to 4 (10−60%). This ichnofabric includes an assemblage composed of diverse ichnofossils. *Tisoa siphonalis* is the most abundant ichnotaxon and accounts for most of the bioturbation in this ichnofabric (Fig. 14a). Some subordinate ichnotaxa are also recorded. The deepest

◂**Fig. 9** Facies types (FT7−FT9, FT11). **a** FT7, hummocky cross-stratified sandstone showing fine-grained, subangular to subrounded, well-sorted, closely-packed quartz arenite cemented by clay and iron oxide, WA86. **b**, **c** FT8, heterolithic cross-bedded sandstone/mudstone. **b** Fine- to medium-grained, subangular to subrounded, loosely-packed quartz arenite with patches of clay, WA84. **c** Laminated mudstone with silt-sized quartz grains embedded in clay matrix, WA81. **d**, **e** FT9, ripple laminated sandstone/siltstone. **d** Very fine- to coarse-grained, subrounded, mono and polycrystalline, siliceous quartz arenite. Quartz grains show corrosion, WA113. **e** Laminated siltstone dominated by silt-sized quartz grains and clay matrix with iron oxide cement, WA88. **f** FT11, organic-rich mudstone showing dark appearance of the clay with organic matter, WA118. All photographs PPL, except for **c**−**e**, which XPL. Scale bars = 0.5 mm, except for **a** and **f**, for which it represents 0.2 mm

tier in the sediment was occupied by the ichnogenus *Tisoa*, whereas *Arenicolites*, *Planolites*, *Palaeophycus*, *Lockeia* and *Ptychoplasma* represent the shallow-tier trace fossils. *Tisoa*-dominated ichnofabrics have been recorded in the middle Bathonian of the Russian platform (Desai et al. 2021) and the upper Jurassic Fensfjord, Sognefjord (Kimmeridgian) and Ula formations (Kimmeridgian−Tithonian) in the Norwegian Sea (Knaust 2019).

Schaubcylindrichnus ichnofabric (Fig. 14b)

This ichnofabric characterises the lower part of unit III (lower Permian) (Fig. 3). Its host rocks are mostly sandstone, shale, mudstone, fossiliferous dolomitic sandstone and fossiliferous sandy dolomite interbeds. This ichnofabric is characterised by a sparse to low bioturbation intensity (ichnofabric index ranges from 2 to 3). *Schaubcylindrichnus* is the most abundant ichnofossil with subordinate *Arenituba*, *Palaeophycus*, *Planolites*, *Skolithos*, *Zoophycos* and rare *Helminthopsis* (Fig. 14b). Most of these ichnofossils represent a shallow-tier activity (tiers 1–3; sensu Hasiotis 2012). No colonization surfaces have been recognized. *Schaubcylindrichnus*-dominated ichnofabrics have been recorded in the lower−upper Jurassic of Norway (Knaust 2017), the Palaeogene Grumantbyen Formation of Norway (Øygard 2016) and the Miocene Taliao Formation of north-eastern Taiwan (Löwemark and Hong 2006).

Zoophycos ichnofabric (Fig. 14c)

It characterises the upper part of unit III of the Aheimer Formation. This ichnofabric is associated with sandstone, shale, mudstone, fossiliferous dolomitic sandstone and fossiliferous sandy dolomite interbeds (Fig. 3). Bioturbation intensity is moderate (ichnofabric index ranges from 3 to 4) and diversity of the trace fossil association is moderate to high. No colonization surfaces have been recognized. *Zoophycos* appears to be the most common trace in this ichnofabric, associated with several other ichnotaxa (Fig. 14c). Generally, the ichnofossils in this ichnofabric, with higher abundance and moderate diversity, are mainly composed of trails on the bedding plane and a few fodinichnia near the bedding plane, locally crosscutting each other. Most trace fossils (about 70%) such as *Phycodes*, *Cruziana*, *Rusophycus*, *Planolites* and *Palaeophycus* occupy the shallower horizons (tiers 1–3). However, *Zoophycos* represents the shallow-middle tier of this ichnofabric. In addition, very shallow tiers to superficial traces (e.g., *Gordia* and *Circulichnis*) are common and produced almost no disturbance of the primary fabric. The *Zoophycos* ichnofabrics are a common component of the distal expression of the *Cruziana* ichnofacies in many Palaeozoic successions, e.g., the Chefar El Ahmar Formation (Devonian) of Algeria (Bouchemla et al. 2021), the middle Permian of Oman (Knaust 2009), the lower Permian Taiyuan Formation of central China (Hu and Qi 2000) and the Hongguleleng Formation (Devonian–Carboniferous transition) of western Junggar, NW China (Fan and Gong 2016).

Discussion

The present study differs from others in integrating, for the first time, different stratigraphical, sedimentological and ichnological information in order to arrive at an accurate insight into the palaeoenvironmental characterisation of the Aheimer Formation. The additional granularity seems to be as a result of the inclusion of ichnological data (Table 4), confirming the finer resolution of the present study.

Palaeoenvironments and palaeoecology

Outcrops in the NGP, including the type section studied, are evidently of younger Carboniferous (Westphalian−Stephanian) and Early Permian ages (Tables 1, 2). These siliciclastic-dominated deposits reflect a marginal depositional site (Tables 3, 4; Fig. 15). The close proximity of the study area to the shoreline (Fig. 1d) is inferred due to the indications of a strong siliciclastic input (Fig. 3). Lithofacies analyses have revealed that this formation was laid down across a relatively wide spectrum of depositional environments, including shallow subtidal, prograding shoreline and fluvial conditions (Table 3), reflecting different stacking patterns of facies in the available accommodation space (Fig. 5a). As mentioned above, the studied succession is subdivided into four 3rd-order sequences. The most important depositional features and environmental parameters governing the distribution of trace fossils, macrofauna and flora are discussed below.

Table 4 Ichnotaxa identified in the upper Carboniferous–lower Permian Aheimer Formation. Information includes occurrence, age, short description, environmental distribution, ethology and the probable trace makers

Ichnotaxon	Occurrence/age	Short description	Environmental distribution	Ethology and probable trace makers
Arenicolites isp. (Fig. 10a)	Unit I (Late Carbo.)	Simple, U-shaped, vertical burrows without spreiten, perpendicular to bedding plane	Eurybathic trace fossil recorded in diverse environments (e.g., Pemberton et al. 2001)	Considered as a dwelling and feeding structure of suspension-feeding annelids (Bromley 1996), among others
Arenituba isp. (Fig. 10b)	Unit III (Early Permian)	Numerous slender, horizontal, straight or slightly curved, sometimes branched tubes, radiating around a central gallery. Tubes filled with fine-grained sandstone with a smooth to finely annulated surface. The burrow fill is structureless, similar to the host rock and sand-packed	Facies-crossing form, restricted to marine environment, occurring in both shallow (Chamberlain 1971) and possibly deep-water marine habitat (Miller 1986)	Interpreted as a combined dwelling and feeding structure where the organism extended itself in search of food (Chamberlain 1971; Stanley and Pickerill 1995)
Circulichnis isp. (Fig. 10c)	Unit III (Early Permian)	Horizontal, approximately circular to oval, cylindrical ring	Facies-crossing form that occurs in both marine and non-marine setting (Buatois and Mángano 1993); shallow (e.g., Fillion and Pickerill 1984) and deep-water marine deposits (e.g., McCann and Pickerill 1988)	A feeding structure (Fodinichnia) probably produced by vermiform animals. Trace makers belong mostly to polychaetes in marine sediments and to oligochaetes in continental sediments (Uchman and Rattazzi 2019)
Cruziana isp. (Fig. 10d)	Unit III (Early Permian)	Elongate, typically ribbon-like, bilobate interface burrows or trails preserved as furrows with median ridges when preserved in concave epirelief (or bilobate trails with median groove when preserved in counterpart convex hyporelief), or paired furrows that are in close proximity (less than the width of a furrow apart)	Typical of the shallow marine *Cruziana* ichnofacies (Baldwin 1977)	*Cruziana* is considered a burrow produced mostly by trilobites (Seilacher 1970) or trilobitomorph arthropods. The intimate association of *Cruziana* and *Rusophycus* (trilobite produced) allows for attribution of the present specimens of *Cruziana* to a similar origin
Diplocraterion parallelum Torell (Figs. 10e, 11c)	Unit I (Late Carbo.)	Vertical, U-shaped, single-spreite burrows; limbs unlined and smooth	Characteristic of settings with strong wave and current energy (Fillion and Pickerill 1990)	Interpreted as a dwelling burrow (domichnia) of suspension-feeding organisms (Fillion and Pickerill 1990)
Gordia aff. *marina* Emmons (Fig. 10f)	Unit III (Early Permian)	Thin, arcuate to winding burrows or trails with self-overcrossing patterns	*Gordia* is a facies crossing form that occurs in both marine and non-marine setting (Gaigalas and Uchman 2004); shallow and deep water marine deposits (Miller and Knox 1985)	This ichnogenus is considered to be a pasichnion or fodinichnion trace, formed within the substrate by a deposit-feeding worm or worm-like organism (Geyer and Uchman 1995)

Table 4 (continued)

Ichnotaxon	Occurrence/age	Short description	Environmental distribution	Ethology and probable trace makers
Helminthopsis isp. (Fig. 10g)	Unit III (Early Permian)	Strong, unbranched, semicircular, loosely meandering ridge, do not touch or cross. Burrow fill is unstructured and similar, coarser or finer in grain size to the surrounding material	Facies-crossing ichnotaxon, common in both marine and non-marine setting; shallow and deep water marine deposits (e.g., Pemberton et al. 2001)	Pascichnia of deposit-feeder organisms, probably polychaete annelids (Bromley 1996; Buatois et al. 1998)
Lockeia siliquaria James (Fig. 10h)	Unit I (Late Carbo.)	Smooth, almond-shaped bulges preserved as low convex hyporeliefs	Eurybathic trace fossil recorded in marine and non-marine environments (Fillion and Pickerill 1990)	These burrows represent temporary resting of bivalve (e.g., Seilacher and Seilacher 1994; Seilacher 2007)
Lockeia isp. (Figs. 10e, i, 11a)	Unit I (Late Carbo.)	Amygdaloidal- to ovoid-shaped mounds (convex hyporelief) or depressions (concave epirelief) that taper at one or both ends; surface usually smooth but may be irregular	Eurybathic trace fossil recorded in marine and non-marine environments (Fillion and Pickerill 1990)	Represents short-lived resting traces (cubichnia) of small burrowing bivalves, perhaps semi-sessile forms (Bromley 1996; Buatois et al. 1998)
Neoeione moniliformis (Tate) (Fig. 11b)	Unit I (Late Carbo.)	Horizontal to sub-horizontal, densely aligned knobby sediment aggregates, which appear along the upper bedding plane as characteristic beaded strings	It is mainly related to a shallow-marine environment (Boyd and McIlroy 2018; Gutiérrez-Marco et al. 2019)	Fodichnia of a deposit-feeding organism (Boyd and McIlroy 2018)
Neonereites multiserialis Pickerill and Harland (Fig. 11c)	Unit I (Late Carbo.)	Straight, irregularly or regularly winding chains of generally loose or interconnected pustules, pods or knobs when preserved in positive relief on lower bedding plane surfaces or corresponding dimples, more rarely pustules, pods or knobs, on upper bedding plane surfaces	The ichnogenus *Nereites* is an eurybathic form and is a common component of Paleozoic shallow-marine facies	Fecal pellet-filled grazing trail or burrow of a deposit feeder. Worms, gastropods, arthropods are possible trace maker
Palaeophycus isp. (Fig. 11a, d)	Unit I, III (Late Carbo.– Early Permian)	Branched or unbranched, smooth or ornamented, lined, essentially cylindrical, predominantly horizontal trace fossils of variable diameter; tube infill typically structureless, of the same lithology as the host rock	Eurybathic trace fossil recorded in diverse environments (e.g., Pemberton et al. 2001)	Domichnia of a deposit feeder or predator, either worm-like organisms or arthropods (Pemberton and Frey 1982)
Phycodes aff. *palmatus* Hall (Fig. 10d)	Unit III (Early Permian)	Horizontal hypichnial burrow system with a slightly curved stem, from which four gently curved and closely spaced burrows branch out	It is mainly related to shallow water environments, being characteristic trace fossil of the *Cruziana* ichnofacies, and less frequently found in deep-marine and non-marine conditions (Han and Pickerill 1994)	Fodinichnia (feeding structures) of burrowing marine organisms such as worms

Table 4 (continued)

Ichnotaxon	Occurrence/age	Short description	Environmental distribution	Ethology and probable trace makers
Planolites isp. (Figs. 10e, 11e)	Unit I, II, III (Late Carbo.– Early Permian)	Cylindrical, smooth walled, unlined, horizontal to undulant, straight to gently curved, unbranched and oriented more or less parallel to the bedding plane; fills typically differ in color from surrounding sediments	Eurybathic trace fossil recorded in marine and non-marine environments (e.g., Pemberton et al. 2001)	Interpreted as a feeding structure of a deposit feeder, mainly worms that actively fill their burrows (Pemberton and Frey 1982)
Protovirgularia isp. (Fig. 11f)	Unit III (Early Permian)	Bilobate horizontal to subhorizontal cylindrical burrow with a straight to slightly curving median ridge and regular to irregular small V-shaped (chevron-like) markings	Cosmopolitan trace fossil in marine and continental Phanerozoic deposits (Knaust 2022)	Encompasses locomotion (repichnion), grazing (pascichnion), resting (cubichnion) and feeding (fodinichnion) (Seilacher and Seilacher 1994; Mángano et al. 2002) of annelids, molluscs and arthropods (Knaust 2022)
Ptychoplasma cf. *excelsum* Fenton and Fenton (Fig. 11g)	Unit I (Late Carbo.)	Nearly smooth, undulating, continuous to discontinuous subhorizontal ridges that display a characteristically amygdaloid, carinate or blocky cross section	*Ptychoplasma* common in shallow marine settings	Resting traces (cubichnia). It is generally associated in the same beds, and commonly the same bedding planes, as various ichnospecies of the bivalve resting trace *Lockeia* (Uchman et al. 2011)
Rhizocorallium isp. (Fig. 11h)	Unit III, IV (Early Permian)	U-shaped spreiten-burrows, parallel or oblique to bedding plane; limbs more or less parallel and distinct	Both shallow and deep-marine environments (Mángano et al. 2002)	Fodinichnia; a suspension and deposit feeding burrow, most likely of crustaceans, polychaetes, and insects (Knaust 2013)
Rusophycus cf. *carbonarius* (Fig. 11i)	Unit III (Early Permian)	Short, interfacial bilobate burrow or surface mark resembling a coffee-bean	Common component of the *Cruziana* ichnofacies under shallow marine conditions (Fillion and Pickerill 1990)	Resting traces (cubichnia) of trilobites (Seilacher 2007), but most likely of searching for food (Neto de Carvalho 2006)
Schaubcylindrichnus freyi Miller (Fig. 11j)	Unit III (Early Permian)	Endichnial, isolated groups or bundles of congruent, lined tubes that ordinarily do not branch or interconnect	Shoreface to upper offshore, developed under normal salinity conditions (Pemberton et al. 2001)	Trace maker is a suspension-feeder organism with the ability to produce the migration of the tube (Löwemark and Hong 2006)
Skolithos linearis (Haldeman) (Fig. 12a, b)	Unit III (Early Permian)	Vertical to slightly inclined, cylindrical to sub-cylindrical, straight to slightly curved, unbranched burrow, more or less distinctly lined, with homogeneous fill and very high length-to-diameter ratio	Shallow marine environments (Fillion and Pickerill 1990)	*Skolithos* is generally interpreted as the domichnion of a suspension-feeding worm or phoronid (Pemberton et al. 2001)
Skolithos isp. (Fig. 12c)	Unit III (Early Permian)	Single vertical and sub-vertical lined burrows having an infill identical to the host rock	Facies-crossing ichnotaxon	Dwelling structures (domichnia) of worms, phoronids, and insect larvae. Arthropods, small vertebrates are also possible trace maker

Table 4 (continued)

Ichnotaxon	Occurrence/age	Short description	Environmental distribution	Ethology and probable trace makers
Thalassinoides paradoxicus (Woodward) (Fig. 12d)	Unit III (Early Permian)	Sparsely to densely but irregularly branched, subcylindrical to cylindrical burrows oriented at various angles with respect to bedding; T-shaped intersections are more common than Y-shaped bifurcations	Mostly registered in shallow-marine environment, usually oxygenated, soft but fairly cohesive substrates (Bromley 1996)	A combined dwelling and feeding burrow systems of decapod crustaceans (e.g., El-Sabbagh et al. 2017)
Th. Suevicus (Rieth) (Fig. 12e, f)	Unit I, III (Late Carbo.– Early Permian)	Predominantly horizontal, more or less regularly branched, essentially cylindrical components forming large burrow systems; dichotomous bifurcations more common than T-shaped branches	Facies-crossing ichnotaxon, common in shallow-marine environments, but also in deep-marine settings (Uchman 1995)	Usually attributed to the activity of suspension- and deposit-feeder decapod crustaceans (Pemberton et al. 2001)
Treptichnus isp. (Fig. 10b)	Unit I, III (Late Carbo.– Early Permian)	Chains of zigzag, straight or curved burrow-segments associated with vertical or oblique tubes comprising three-dimensional structures	Eurytopic form of behavior; it has been recorded from lacustrine (Archer and Maples 1984), brackish tidal flat (Rindsberg 1990), shallow marine (Fedonkin et al. 1983), bathyal (Seilacher and Hemleben 1966), and submarine fan environments (Crimes et al. 1981)	*Treptichnus* is interpreted as both a feeding structure (Seilacher and Hemleben 1966) and a farming trace (Rindsberg 1990), made by vermiform animals (Buatois et al. 1998)
Tisoa siphonalis Serres (Fig. 12g–i, 13a–c)	Unit I (Late Carbo.)	Simple, vertical, rarely branched, U-shaped burrows having closely appressed limbs, basal part of "U" rarely preserved; thus, specimens consist typically of two parallel tubes	Shallow to deep marine environments (Knaust 2017, 2019)	Interpreted as a dwelling structure (domichnia) of tube-dwelling polychaetes
Zoophycos isp. (Fig. 13d–f)	Unit III, IV (Early Permian)	Spreite structures composed of numerous small, more or less U- or J-shaped protrusive burrows of variable length and orientation. Spreite arranged in helicoid spirals with an overall outline of circular, elliptical or lobate shape; central vertical tunnel or marginal tube may be present	Eurybathic, typical of fine-grained substrates characterized by low sedimentation rates	Attributed to the deposit-feeding activity of polychaetes (Bischoff 1968) and sipunculids (Wetzel and Werner 1981), to the imprints of prostomia of sabellids (Plička 1969) and even the feeding activity of umbellulids (Pennatulaceids) (Bradley 1973)

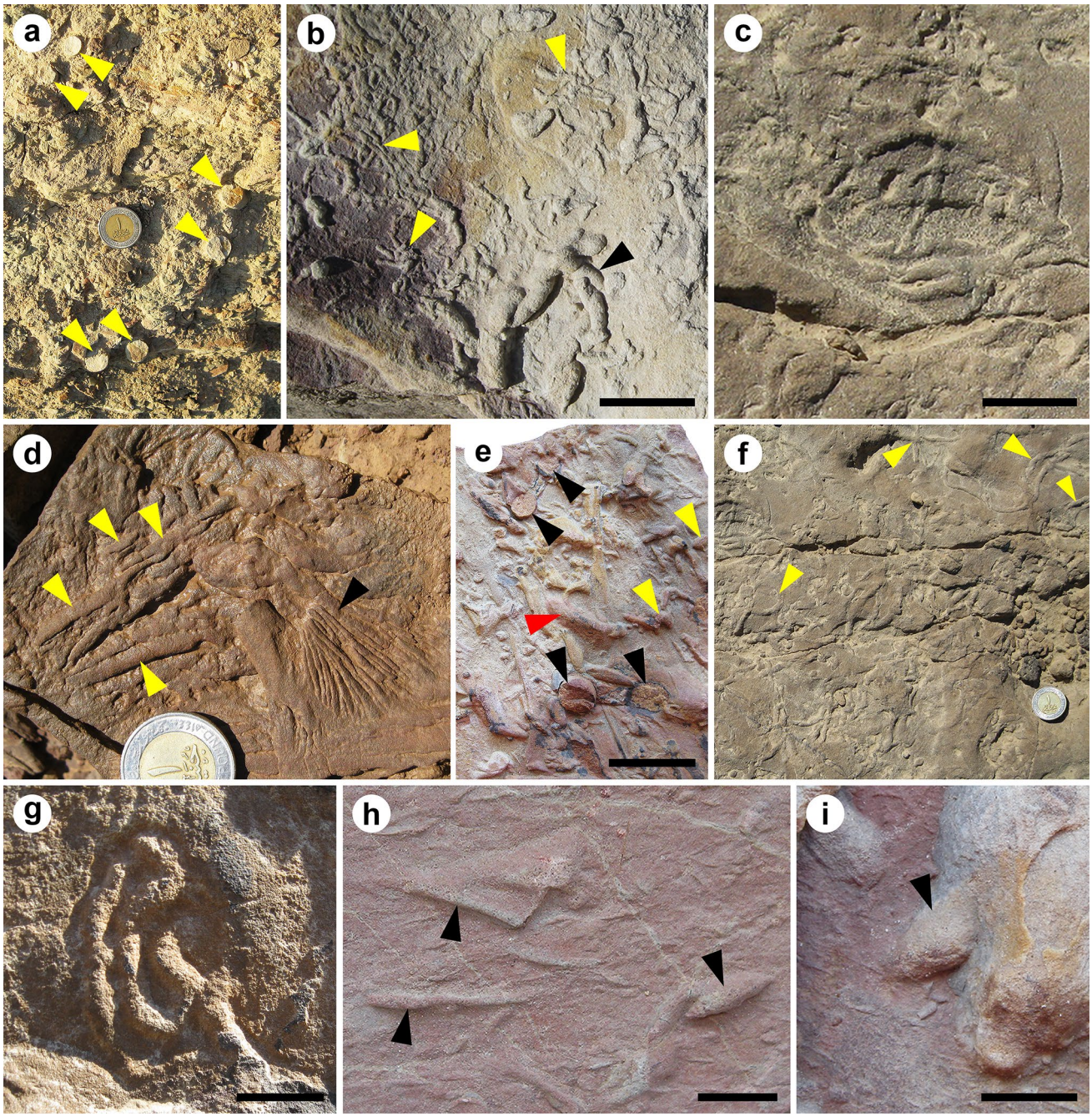

Fig. 10 Trace fossils from the upper Carboniferous–lower Permian Aheimer Formation. **a** Siltstone bedding plane with few cross-sections (arrows) of the sand-filled *Arenicolites* isp., unit I. **b** Sandstone bedding plane with burrows of *Arenituba* isp. (yellow arrows) co-occur with *Treptichnus* isp. (black arrow), unit III. **c** Sandy dolomite bedding plane with *Circulichnis* isp., unit III. **d** Dolomitic ferruginous sandstone with *Cruziana* isp. (yellow arrows) co-occur with *Phycodes* aff. *palmatus* (black arrow) oriented parallel to bedding, unit III. **e** Dolomitic sandstone with traces of *Diplocraterion parallelum* (black arrows) co-occur with *Lockeia* isp. (yellow arrows) and *Planolites* isp. (red arrow), oriented parallel to bedding, unit I. **f** Sandy dolomite bedding plane with numerous *Gordia* aff. *marina* (arrows), unit III. **g** Sandstone bedding plane with traces of *Helminthopsis* isp., unit III. **h** Ferruginous siltstone with *Lockeia siliquaria* bulges (arrows) oriented parallel to bedding, unit I. **i** Bedding plane of ferruginous siltstone with an ovoid-shaped mound of *Lockeia* isp. (arrow), unit I. Scale bars = 2.0 cm, except for **h** and **i**, for which it represents 1.0 cm

Depositional sequence NG 1 (upper carboniferous)

The HST deposits of this sequence are represented by a single facies association (FA1), including two facies types (FT1 and FT2) (Table 3; Figs. 3, 5a). These fine-grained siliciclastic and dolomite facies types show a marine

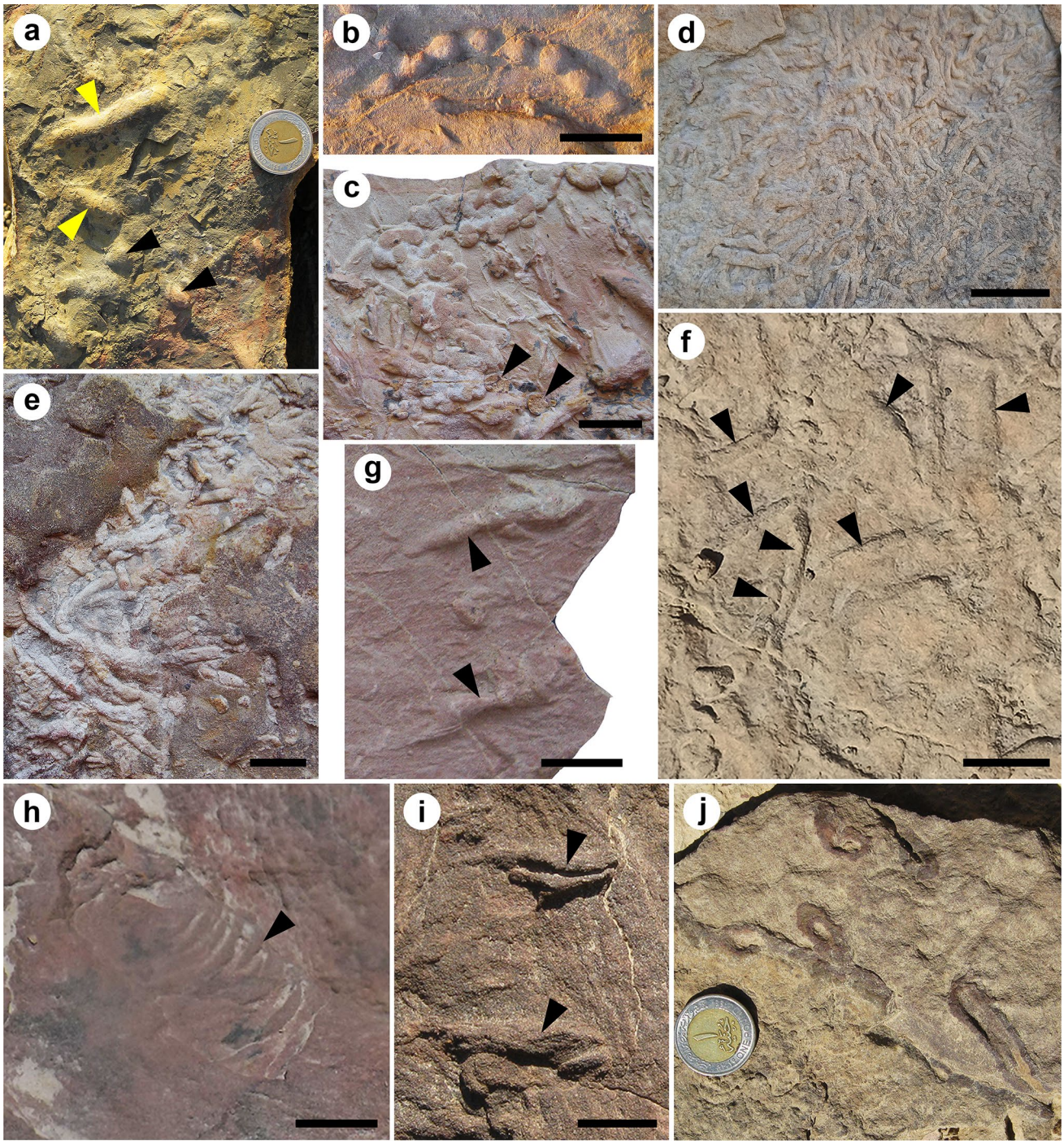

Fig. 11 Trace fossils from the upper Carboniferous–lower Permian Aheimer Formation. **a** Fine-grained sandstone with traces of *Lockeia* isp. (black arrows) co-occur with *Palaeophycus* isp. (yellow arrows) mostly oriented parallel to bedding, unit I. **b** Siltstone with a beaded string of *Neoeione moniliformis*, unit I. **c** Bedding plane of ferruginous siltstone with numerous interconnected pustules of *Neonereites multiseriali* co-occur with *Diplocraterion parallelum* (arrows), unit I. **d** Fine-grained sandstone bedding plane with abundant tubes of *Palaeophycus* isp., unit III. **e** Ferruginous sandstone bedding plane with numerous passive sand-filled traces of *Planolites* isp., unit I. **f** Dolomitic sandstone bedding plane with high density traces of *Protovirgularia* isp. (arrows), unit III. **g** Ferruginous siltstone with few ridges of *Ptychoplasma* cf. *excelsum* (arrows) oriented parallel to bedding, unit I. **h** Dolomitic ferruginous sandstone bedding plane with *Rhizocorallium* isp. (arrow), unit III. **i** Dolomitic ferruginous sandstone bedding plane with few traces of *Rusophycus* cf. *carbonarius* (arrows), unit III. **j** Bedding plane of sandstone with horizontal, vertical, and sub-vertical tubes of *Schaubcylindrichnus freyi*, unit III. Scale bars = 1.0 cm, except for **b**–**d** and **f**, for which it represents 2.0 cm

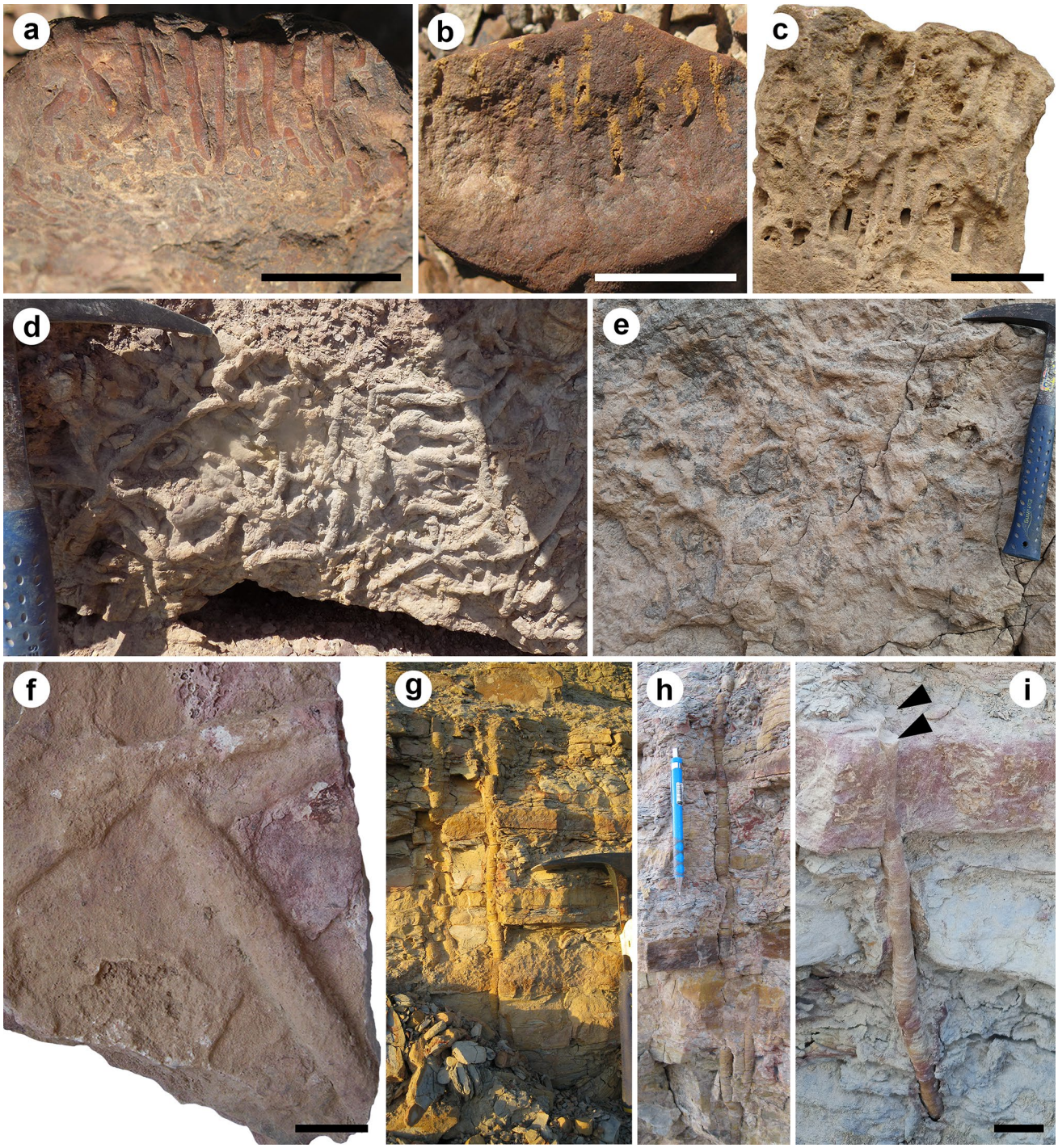

Fig. 12 Trace fossils from the upper Carboniferous−lower Permian Aheimer Formation. **a**−**c** Sandy dolomite with numerous burrows of *Skolithos linearis* (**a**, **b**) and *Skolithos* isp. (**c**) oriented perpendicular to bedding, unit III. **d** Cross-section view of sandstone with a complex burrowing system of *Thalassinoides paradoxicus*, unit III. **e**, **f** Bedding plane of sandstone with *Th. suevicus* burrows, unit III and I, respectively. **g**−**i** Shale and siltstone with sandstone interbeds penetrated by elongate paired burrows of *Tisoa siphonalis*, unit I. Note the moderately preserved horizontal lamination in passive sand fill. Paired burrows descend mainly from the upper surface of siltstone layers (arrows in **i**). Scale bars = 2.0 cm

environment, ranging from intertidal to shallow subtidal settings (Fig. 15). The tidal effect throughout deposition is supported by the occurrence of highly ferruginous sandstone/shale couplets, and the existence of wave-ripples, cross-lamination, and mudstone drapes in sandstone (e.g., Buatois and Mángano 2003). The pattern of facies repetition with nearly

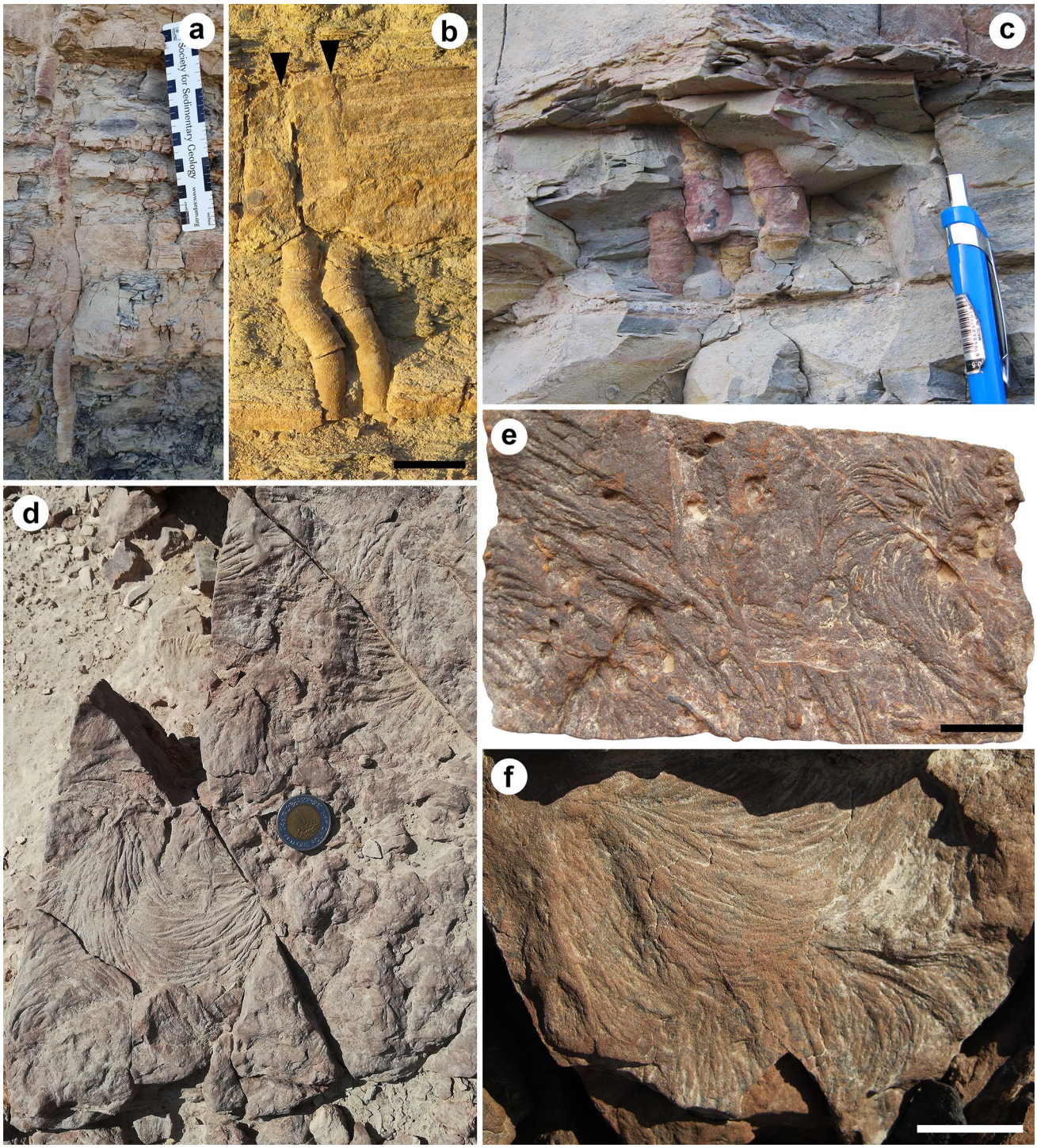

Fig. 13 Trace fossils from the upper Carboniferous−lower Permian Aheimer Formation. **a**, **b** Shale and siltstone with sandstone interbeds penetrated by elongate paired *Tisoa siphonalis* burrows with slight helical course and passive sand fill. Paired burrows descend mainly from the upper surface of siltstone layers (arrows in **b**), unit I. **c** Shale penetrated by passive sand-filled, paired burrow parts of *Tisoa siphonalis*, unit I. **d**−**f**. Bedding plane of dolomitic ferruginous sandstone with burrows of *Zoophycos* isp., unit III. Scale bars = 2.0 cm

equal thickness of sets of strata (Figs. 4b, 5a, b, 6a) confirms an aggrading shelf with equal rates of accommodation and sedimentation (Van Wagoner et al. 1990). In addition, the cyclical thickening and thinning may reflect differences in tidal current energy during neap-spring tidal fluctuations (Kvale et al. 1989; Kvale and Archer 1990).

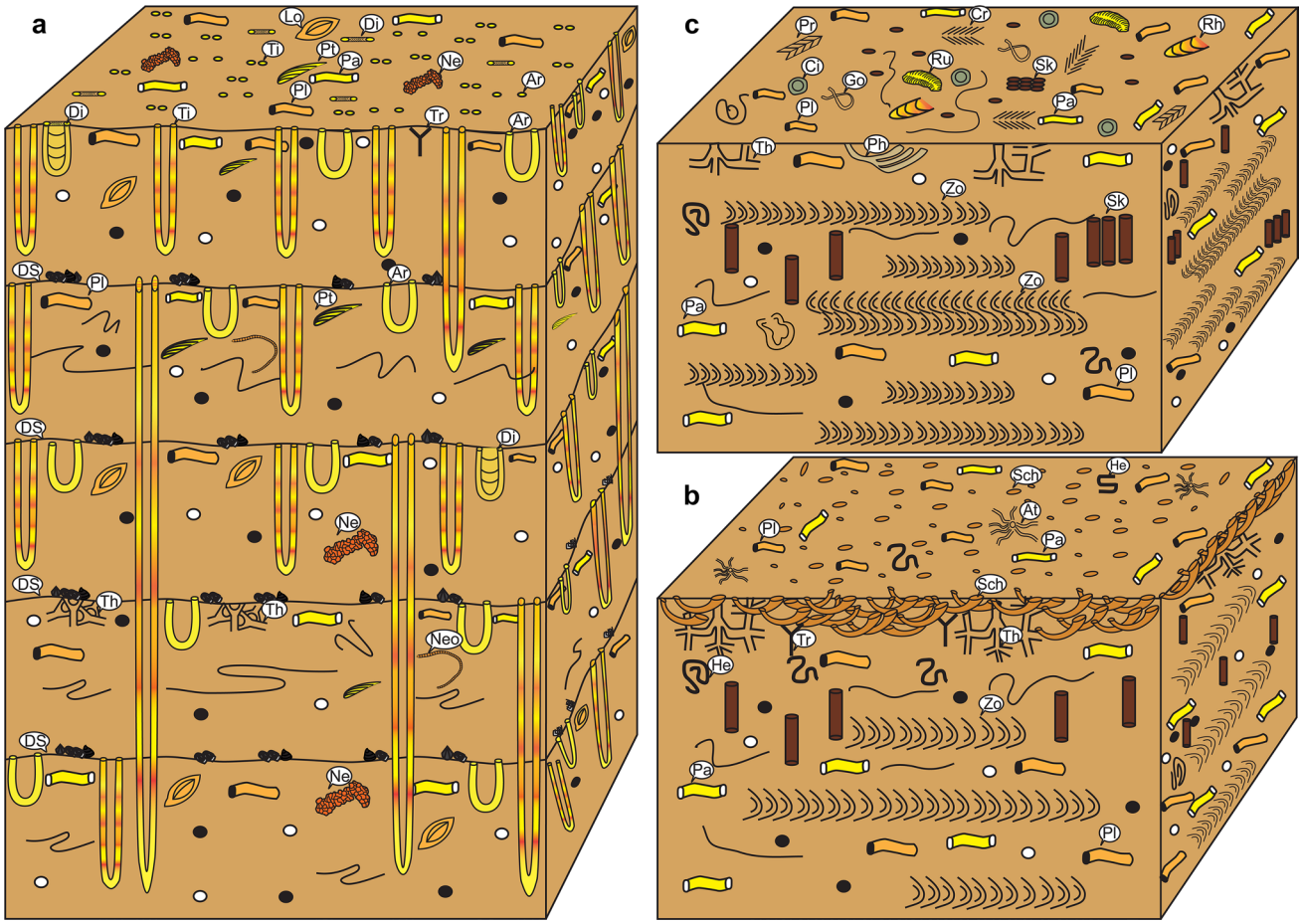

Fig. 14 Schematic diagrams (not to scale) of the described ichnofabrics in the Permo–Carboniferous Aheimer Formation, western side of the Gulf of Suez, Egypt. **a** *Tisoa* ichnofabric. **b** *Schaubcylindrichnus* ichnofabric. **c** *Zoophycos* ichnofabric. Abbreviation: Ar: *Arenicolites*; At: *Arenituba*; Ci: *Circulichnis*; Cr: *Cruziana*; Di: *Diplocraterion*; Go: *Gordia*; He: *Helminthopsis*; Lo: *Lockeia*; Neo: *Neoeione*; Ne: *Neonereites*; Pa: *Palaeophycus*; Ph: *Phycodes*; Pl: *Planolites*; Pr: *Protovirgularia*; Pt: *Ptychoplasma*; Rh: *Rhizocorallium*; Ru: *Rusophycus*; Sch: *Schaubcylindrichnus*; Sk: *Skolithos*; Th: *Thalassinoides*; Tr: *Treptichnus*; Ti: *Tisoa*; Zo: *Zoophycos*; DS: Discontinuity surface

The occurrence of organic-rich fissile shale may suggest a partially restricted shallow subtidal marine environment with a low to moderate rate of sedimentation (e.g., Pemberton et al. 1992). In addition, the recorded small-scale oscillation ripples and combined flow ripples also indicate periods of standing water and wave modification. This restricted condition helped in reducing the wave action (i.e., low to moderate water energy), and consequently, permits accumulation of organic material in bottom sediments. In these restricted environments, which are characterised by the increase of nutrient supply in the water column and fine-grained sediment, the seafloor and bottom sediments may become oxygen-deficient (i.e., dysoxic conditions; cf. Jarvis et al. 1988; Koutsoukos et al. 1990; Fürsich et al. 2012). These conditions may be also documented by the low to moderate species diversity of macrofossils (mainly brachiopods and crinoids) and microfossils (mainly agglutinated and microgranular benthic foraminifera). In addition, the near absence of infaunal elements may also reflect these dysoxic conditions (cf. Oschmann 1993; Fürsich et al. 2012). In these stressed conditions, the *Tisoa* trace maker may burrow deeply into anoxic sediments for deriving energy via chemosymbiosis and consequently produce extraordinary depths (Knaust 2019; present study).

As was mentioned, sediments of DS NG 1 are intensively burrowed (Table 4; Fig. 3). The abundant traces of suspension-feeding organisms support at least moderate water energy that keeps organic nutrients in suspension (i.e., a low to moderate rate of sedimentation). At the same time, this level of water energy permits the accumulation of food particles for different deposit-feeding trace makers of several ichnotaxa. The occurrence of large-diameter *Thalassinoides* points to a nutrient-rich and well-oxygenated water column along with low- to moderate-energy conditions (e.g., Abdel-Fattah et al. 2016; El-Sabbagh et al. 2017; Vinn et al. 2020). However, shrimp-produced *Thalassinoides*

had a broader range of salinity tolerance, ranging well into environments of low salinity (e.g., Swinbanks and Luternauer 1987). Horizontal burrows of *Treptichnus* ichnotaxon suggest low-energy conditions on the marine shelf (Buatois et al. 2013). The latter is also confirmed by the absence of the more basinal marine expressions (e.g., *Rhizocorallium* and *Zoophycos*) and/or high-energy proximal suites (e.g., *Skolithos*). *Diplocraterion* ichnospecies have been found in tidal flats and estuaries (e.g., Buatois and Mángano 2011; Gingras et al. 2012a). In these aspects, their producer is considered as an opportunistic species (e.g., *r*-strategist) that thrived in stressful brackish-water conditions (Knaust 2017). The latter is also confirmed by the occurrence of some agglutinated genera as *Ammobaculites*, *Trochammina* and *Reophax* (Kureshy 1966; Armstrong and Brasier 2005).

Based on the works of Seilacher (1964, 1967a, b) and Frey and Seilacher (1980), all of the recorded ichnogenera correspond to a firmground suite of the *Glossifungites* Ichnofacies, representing colonization of exhumed firm but unlithified substrates, and greatly resembling the intermediate energy firmground suites of MacEachern et al. (2007b). Although suites attributable to the *Glossifungites* Ichnofacies occur in a wide range of environments (Hayward 1976; Frey and Seilacher 1980; Savrda 1991; MacEachern et al. 1992a, b; Raychaudhuri et al. 1992; MacEachern and Burton 2000; Gingras et al. 2002a, b; Bann et al. 2004; Dasgupta and Buatois 2012), the trace fossil suite in this ichnofacies, dominated with long, narrow vertical tubes, and usually paired, is common in nearshore environments, particularly in intertidal sediments (e.g., Rhoads 1967; Zonneveld et al. 2001). These findings are consistent with our results. The trace makers require the substrate to be exhumed by mechanical removal of loose unconsolidated overburden in order to reach the firm substrate (e.g., MacEachern et al. 1992a, b; Buatois and Mángano 2011). Consequently, this leads to the development of a discontinuity surface, i.e., short-lived omission (e.g., MacEachern et al. 1992a; Pemberton et al. 2001). In the study area, a total of five autogenic *Glossifungites* Ichnofacies-demarcated siltstone surfaces (sensu Abdel-Fattah et al. 2016) were recognized in sediments of DS NG 1. After subaerial exhumation and/or submarine erosion, the colonization stage of the discontinuity surface by firmground trace makers is performed during periods of marine conditions (i.e., a hiatus in deposition). Subsequently, passive filling of the burrows is completed during an ensuing depositional episodes and burial of the firmground suite.

Depositional sequence NG 2 (lower Permian)

As was mentioned, this sequence consists of three systems tracts: LST, TST and HST, comprising the entire unit II and the lower part of unit III (Fig. 5a). The LST sediments are represented by a single facies association (FA2) that includes two facies types (FT3 and FT4) (Table 3; Fig. 3). The presence of trough and planar cross-bedding, fining-upward cycles and an erosive lower boundary supports these stacked deposits as low-sinuosity braided channels (Postma 1990; Galloway and Hobday 1996; Miall 1996). Pebbly and coarse-grained sandstones are interpreted as channel fills deposited by tractive currents, whereas the fine-grained sandstone and siltstone are deposited during the stage of falling flow velocity of the flood on the channel banks (Dalrymple et al. 1990; Miall 1996). In addition, kaolinitic siltstones could be related to changes in climate to a wet period and retrogradational time (Kämpf and Schwertmann 1983).

The large and rounded exotic quartz pebbles and gravels characterise the lower part of the LST of this sequence seem to be derived from quartz veins occurring within the Precambrian basement and transported northward for a long distance. It is worth mentioning that, within the Palaeozoic succession of the northern part of the Eastern Desert of Egypt, similar large pebbles are only recorded in the basal part of the Cambrian sandstone of the Araba Formation at Somr El Qaa (around 28°13'N and 32° 22'E) (Klitzsch et al. 1990). The latest Carboniferous and earliest Permian tectonic instability played an important role in the influx of these coarse clastics with high rates of deposition (e.g., Klitzsch 1990; Klitzsch et al. 1990).

Within these LST sediments, pith casts of *Calamites* are recorded (Fig. 4d). *Calamites* grew to 20 m tall, standing mostly along the sandy banks of rivers (Rafferty 2011). In addition, a distinctly different ichnocoenosis is represented within this unit by the monospecific occurrence of a small population of *Planolites* isp. (Fig. 3), which, in this context, indicates a stressed, opportunistic colony (Ekdale 1985; Bromley 1996). Freshwater discharge was conducive to limit biogenic activity, resulting in reduced trace fossil diversity and sparse burrowing (e.g., Bhattacharya and MacEachern 2009). In addition, the absence of marine micro- and macrofossils in sediments of this LST confirms these environmental conditions (Fig. 15).

In general, sediments of both TST and HST of DS NG 2 consist of sandstone, siltstone, mudstone and dolomite interbeds, representing mainly the third facies association (FA3) and including five facies types (FT5–FT9; Figs. 3, 5a). Furthermore, these sediments are characterised by abundant sedimentary structures, highly burrowed and fossiliferous with micro- and macro- fossils (Tables 3, 4; Fig. 3). These results confirm depositional palaeoenvironments ranging from upper shoreface to the offshore transition (Fig. 15). Sandstones with large-scale tabular-planar cross-bedding, trough cross-bedding and symmetrical wave ripples can be deposited throughout the upper shoreface (Clifton 2006). Sandstones and siltstones showing large-scale hummocky cross stratification and oscillation ripples mark the lower to

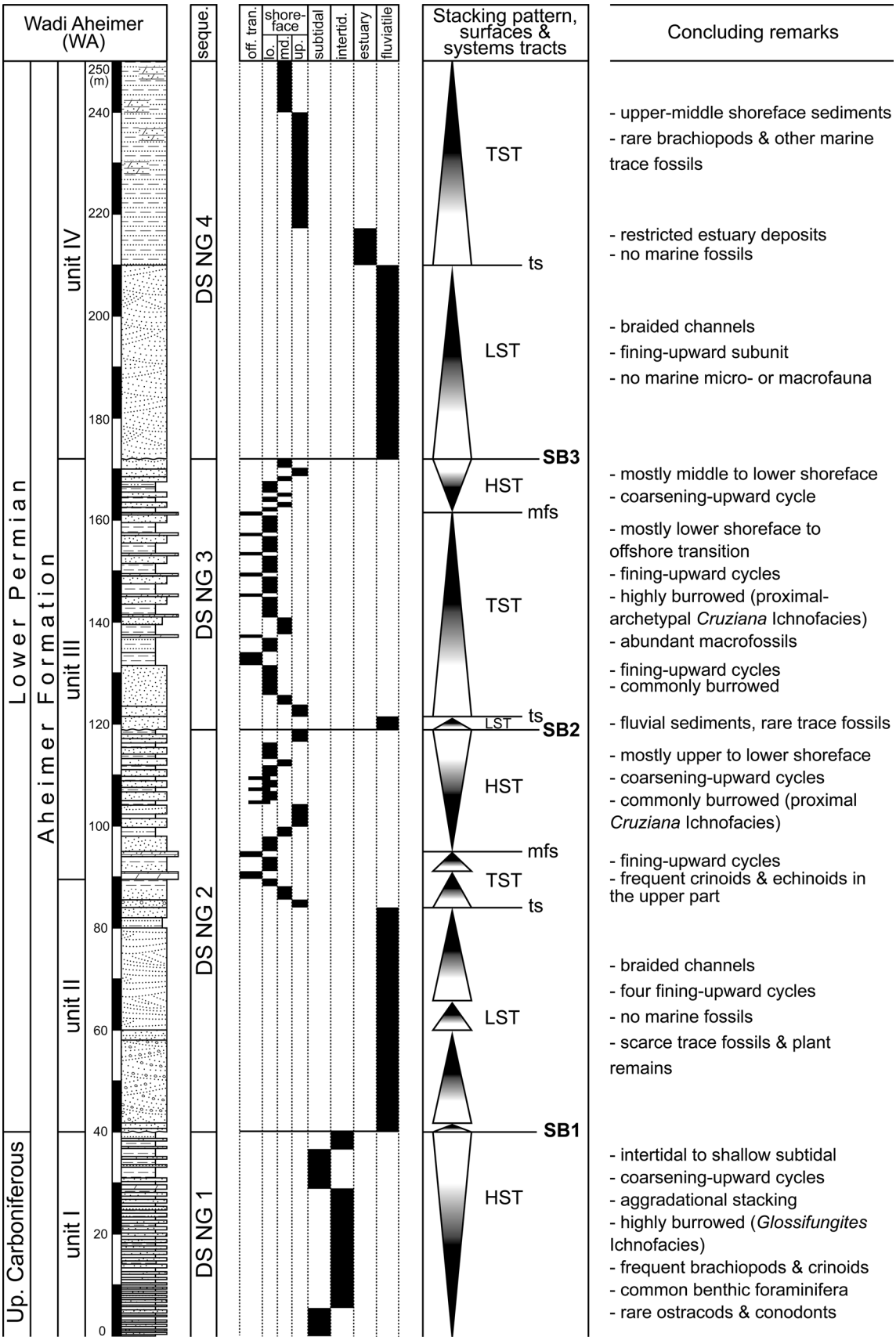

Concluding remarks

- upper-middle shoreface sediments
- rare brachiopods & other marine trace fossils

- restricted estuary deposits
- no marine fossils

- braided channels
- fining-upward subunit
- no marine micro- or macrofauna

- mostly middle to lower shoreface
- coarsening-upward cycle

- mostly lower shoreface to offshore transition
- fining-upward cycles
- highly burrowed (proximal-archetypal *Cruziana* Ichnofacies)
- abundant macrofossils

- fining-upward cycles
- commonly burrowed

- fluvial sediments, rare trace fossils

- mostly upper to lower shoreface
- coarsening-upward cycles
- commonly burrowed (proximal *Cruziana* Ichnofacies)

- fining-upward cycles
- frequent crinoids & echinoids in the upper part

- braided channels
- four fining-upward cycles
- no marine fossils
- scarce trace fossils & plant remains

- intertidal to shallow subtidal
- coarsening-upward cycles
- aggradational stacking
- highly burrowed (*Glossifungites* Ichnofacies)
- frequent brachiopods & crinoids
- common benthic foraminifera
- rare ostracods & conodonts

◂**Fig. 15** Lithostratigraphy, interpreted depositional environments, sequence stratigraphy and concluding remarks of the upper Carboniferous-lower Permian Aheimer Formation in the study area

middle shoreface environment (Hunter and Clifton 1982; Clifton 2006). The amalgamation of the oscillatory motion from waves and storm-generated currents are assumed to produce hummocky cross-stratification (Harms et al. 1982; Swift et al.1983; Duke et al. 1991). Burrowed and fossiliferous dolomite with crinoids, brachiopods, bivalves, foraminifera and bryozoan skeletal fragments suggest normal-marine environments ranging from lower shoreface to offshore transition (Table 3). The latter is also confirmed by the lower level of burrowing and the paucity of physical sedimentary structures in the mudstone sediments, documenting deposition below fair-weather wave-base in a quiet-water environment (i.e., offshore transition) (Leckie and Walker 1982; Rosenthal and Walker 1987; MacEachern and Pemberton 1992).

Sediments of the upper part of the HST of this depositional sequence are burrowed with a characteristic suite of trace fossils (Figs. 3, 5a, 15), confirming the activity of varied producers that mainly performed different trophic behaviours. This part (between 110 and 118 m; Figs. 3, 5a) contains abundant *Palaeophycus* isp., *Planolites* isp., *Thalassinoides paradoxicus*, *Skolithos* isp. and *Zoophycos* isp., reflecting the activity of deposit (fodinichnia) and suspension (domichnia) feeders (Table 4). Although *Zoophycos* is a common ichnotaxon in deep marine waters of the Mesozoic and later (Ekdale and Berger 1978; Bottjer et al. 1987; Vinn et al. 2020), Palaeozoic *Zoophycos* occurs in nearshore deposits (e.g., Osgood and Szmuc 1972; Yurewicz 1977; Vinn and Toom 2015; Bouchemla et al. 2021). *Skolithos* is typically marine in origin (e.g., Trewin and McNamara 1995). It is a common indicator of relatively high energy, shallow-water, nearshore to marginal-marine environments (e.g., Desjardins et al. 2010; Vinn and Wilson 2013; Knaust 2017). *Palaeophycus* occurs in various palaeoenvironmental marine settings (Frey and Pemberton 1991; Löwemark and Nara 2010; Toom et al. 2019), including shoreface and offshore deposits (Knaust 2017). Consequently, this trace fossil assemblage occurring in the upper part of the HST of DS NG 2 is interpreted as the shallow-marine (middle to lower shoreface) proximal *Cruziana* Ichnofacies (e.g., Seilacher 1967a, b).

Depositional sequence NG 3 (lower Permian)

Similar to the underlying sequence, DS NG 3 consists of three systems tracts: LST, TST and HST, comprising the upper part of unit III (Fig. 15). The LST sediments are devoid of any marine micro- or macro- fossils. However, plant remains and rare traces of *Helminthopsis* isp. have been found (Fig. 3). The recorded *Ginkgo*-like fossil leaves (Fig. 4f) represent a terrestrial plant, which prefers a warm, humid, open-canopy and a well-drained environment (Lin et al. 2022). *Helminthopsis* is a facies-crossing ichnotaxon, common in both marine and non-marine settings (e.g., Pemberton et al. 2001). Their producer, probably polychaete annelids, occurs in brackish to fully marine environments (Bromley 1996; Buatois et al. 1998).

Sediments of both TST and HST of DS NG 3 represent the second and the third facies associations (FA2 and FA3, respectively), including seven facies types (FT3−FT9; Figs. 3, 5a). In addition, these sediments are characterised by moderately abundant sedimentary structures, highly burrowed and highly fossiliferous with macrofossils (Tables 3, 4; Fig. 3), documenting depositional environments ranging from upper shoreface to offshore transition (Fig. 15).

The heterolithic nature of the facies indicates sedimentation in alternating suspension fallout and bed-loads within a low-energy setting below wave base (i.e., deposition in the lower shoreface environment) (Hunter et al. 1979; Leckie and Walker 1982; MacEachern and Pemberton 1992). Sediments of the TST, in particular, are intensively burrowed with a high ichnodiversity (Figs. 3, 5a, 15). These ichnotaxa have been produced primarily by deposit-feeding organisms in addition to suspension feeders and grazers (Table 4). *Cruziana* co-occurs with *Rusophycus* and they are mainly related to shallow-water environments (e.g., Fillion and Pickerill 1990; Seilacher 2007; Vinn 2014; Vinn and Toom 2016). *Phycodes* likewise is commonly recorded in shallow-marine environments (Han and Pickerill 1994). *Palaeophycus* is regarded as a eurybathic trace fossil recorded in diverse environments (e.g., Pemberton et al. 2001). *Circulichnis* is known in marine and non-marine sediments (Fillion and Pickerill 1984; Uchman and Rattazzi 2019). *Gordia* is a facies-crossing form that occurs in both marine and non-marine settings (Gaigalas and Uchman 2004), including shallow and deep-water marine deposits (Miller and Knox 1985). *Schaubcylindrichnus* occurs in a wide range of environments, particularly in lower shoreface deposits (Frey and Howard 1985, 1990). *Rhizocorallium* occurs in nearshore, shelf and deep-marine sediments (e.g., Mángano et al. 2002; Knaust 2017). It represents a common constituent of transgressive systems tracts (e.g., Knaust 1998; MacEachern et al. 2012).

In general, the presence of a diversified trace fossil assemblage, produced primarily by deposit feeders in low- to moderate-energy conditions along with a moderate rate of sedimentation in nutrient-rich sediments, as well as the water column, suggests a typical proximal-archetypal *Cruziana* Ichnofacies (e.g., MacEachern et al. 1999, 2007a). In general, the presence of fully marine trace fossils (e.g., *Cruziana, Rausophycus*, *Rhizocorallium*) with almost homogeneous distribution suggests relatively stable and low-stress

conditions (Gingras et al. 2012b; MacEachern et al. 2010). However, the occurrence of abundant *Zoophycos* in about six levels within the upper part of the TST of DS NG 3 (Figs. 3, 15) may indicate an episodic depletion of oxygen on the seafloor, i.e., dysoxic to anoxic seafloor conditions. Ekdale and Mason (1988) mentioned that fodinichnia-dominated associations (e.g., *Zoophycos*) occur where bottom water is oxic to dysoxic and the interstitial water is anoxic. In general, sediments accumulated in oxygen-poor depositional environments commonly contain trace fossils that have been produced by low-oxygen-tolerant deposit-feeding organisms (e.g., Bromley and Ekdale 1984; Savrda and Bottjer 1986). Furthermore, the oxygen-controlled trace-fossil model of Ekdale and Mason (1988) suggests that the decrease of oxygen concentration of the interstitial water parallels a transition from trace-fossil associations dominated by dwelling traces of suspension feeders (i.e., domichnia) to trace-fossil associations dominated by deposit-feeding structures (i.e., fodinichnia). These observations are in accordance with our results.

Depositional sequence NG 4 (lower Permian)

This sequence consists of several facies types, representing two systems tracts: LST and TST (Figs. 3, 5, 15). This greatly varied microfacies and abundant sedimentary structures document different depositional settings, ranging from fluvial (FT3) in the entire of LST, restricted estuary (FT11) in the basal part of the TST, and shoreface (FT5, FT8, FT9) in the upper part of the TST, and confirming different stacking pattern of facies in the available accommodation space (Fig. 15).

The LST starts with fluvial deposition represented by planar to trough cross-bedded sandstones, and confirming that braided streams dominated the area. Deposition of clean sand can be interpreted as stream bedload continuously cutting their banks, leaving no chance for floodplain fines to be preserved (e.g., Miall 1985, 1993; Galloway and Hobday 1996). The highest degree of channel amalgamation is recognized at the base of fluvial depositional sequences and is caused by a combination of low rates of floodplain aggradation, high rates of lateral channel migration, and high rates of avulsion (Catuneanu et al. 2011; Catuneanu 2017, 2019).

In the basal part of the TST, the organic-rich mudstones are devoid of any marine micro- or macro- fossils. The overlying very thin interbeds of red siltstone and fine-grained sandstone may indicate the presence of subaerial exposures and oxidation (Miall 1985, 1996; Retallack 2001). Consequently, these facies may be deposited in restricted estuaries with alternating low- and moderate-energy conditions (Prothero and Schwab 1996). On the other hand, sandstone and siltstone sediments in the upper part of the TST are characterised by flat and ripple lamination, wave-rippled thin beds and low-angle cross lamination with rare brachiopod imprints and other marine ichnofauna, documenting deposition in the upper to middle shoreface environment (Fig. 15) (Hunter and Clifton 1982; Clifton 2006).

Regional correlations

In Egypt, similar depositional settings have been recorded at several outcrops on the western side of the Gulf of Suez (Tables 1, 2). In the subsurface of the Gulf of Suez region, the Aheimer Formation is correlated with the upper part of the Nubia "B member" of the oil companies' classification (e.g., Hermina et al. 1983). In addition, time-equivalent rocks are likewise known from the subsurface of the northern part of the Western Desert (the Safi Formation; e.g., Keeley 1989). On the eastern side of the Gulf of Suez, in contrast, the absence of the upper Carboniferous−lower Permian Aheimer Formation reflects local uplift caused by tectonic deformation in conjunction with the Hercynian Orogeny (Kora 1984, 1998; Klitzsch 1990; Klitzsch et al. 1990; Issawi et al. 1999; Guiraud et al. 2001, 2005). The Permo−Carboniferous sediments as well as the older deposits were consequently removed by erosion. In general, all these upper Carboniferous−lower Permian successions may represent the last major invasion of the Palaeo-Tethys Ocean into the northern part of Egypt during Palaeozoic times (Bandel and Kuss 1987; Keeley 1989; Klitzsch 1990; Klitzsch et al. 1990).

On the other hand, the studied upper Carboniferous−lower Permian Aheimer Formation can be regionally correlated with the Assedjefar, Dembaba and Tiguenrourine formations of western Libya (Bellini and Massa 1980). The upper part of the Aheimer Formation can be correlated with the lower Permian Saad Formation of southern Israel (Zaslavskaya et at. 1995). In Syria, equivalent Permo-Carboniferous sediments have been described as the Heil Formation (Al-Youssef and Ayed 1992). Equivalent deposits were also recorded in central Saudi Arabia (the Unayzah Formation; Al-Laboun 1987) and in Oman (the Al Khlata and Gharif formations; Levell et al. 1988).

Carboniferous–Permian glaciations

The late Carboniferous− early Permian glaciations in Gondwana were diachronous and affected North Africa and the Middle East region (e.g., Le Heron et al. 2009 and references therein). With the exception of some examples of glacially-related deposits in the Gilf El Kebir region of SW Egypt, i.e., the eastern Sahara (Klitzsch 1983, 1990), all other upper Carboniferous−Permian glacial deposits are only well established in Oman, Yemen and Saudi Arabia (Braakman et al. 1982; Al Husseini 2004; Le Heron et al. 2009). In these regions, ice sheets and glaciers were mainly concentrated

in tectonically uplifted areas at active plate boundaries, i.e., Hercynian uplift (Eyles 1993; Al Husseini 2004).

In the Gilf El Kebir region of SW Egypt, and adjacent to the Libyan border, Klitzsch (1983) described poorly sorted sediments unconformably overlying a Devonian–Stephanian fluvio-deltaic succession. This unit, the Wadi Malik Formation (sensu Klitzsch 1990), is overlain by Jurassic lacustrine deposits. Le Heron et al. (2009, p. 68) stated that "a glacial origin for these poorly sorted deposits remains plausible but has not been subsequently substantiated". Consequently, further fieldwork is required to confirm the glacial origin for these sediments.

No previous studies have identified any evidence for the late Carboniferous− early Permian glaciations in the northern parts of Egypt. However, El-Noamani and Tahoun (2019) reported that the palaeofloral communities recovered from the subsurface upper Palaeozoic Safi Formation in the west Beni Suef Basin of the northern Western Desert of Egypt may confirm a significant effect of a glacial climate. They identified two palaeofloral communities. The first one is represented by a cold climate low- and wet- land fern community. The second palaeocommunity includes an upland palaeoflora that is mainly developed under the influence of lacustrine flooding resulting from minor deglaciation events.

In fact, the reliability of the influence of the late Carboniferous−Permian glacial-interglacial cycles on the studied sedimentary succession in Wadi Aheimer requires further investigation. However, the occurrence of lithologically repetitive successions containing organic-rich fissile shales in the HST of the DS NG 1 (Figs. 3, 4b, 5a, b, 6a) may be attributed to the effect of the late Carboniferous interglacial cycles, representing shallow glaciomarine organic-rich sediments accumulating in topographically depressed areas during transgression (sensu Lüning et al. 2000). In addition, in the Mid-Continent region of North America during the Permo−Carboniferous period, the growth and decay of Gondwanan ice sheets caused large eustatic sea-level fluctuations, resulting in deposition of lithologically repetitive successions. These cyclical sequences include thin core shale deposits, which are enriched in organic matter, trace metals and authigenic phosphate, confirming deposition during glacio-eustatic highstands that resulted in oxygen-deficient bottom waters in this mid-continental sea in that region (Heckel 1986, 1991; Algeo et al. 2004). Alternatively, these black shales in the HST of the studied section may be interpreted as sediments deposited along the maximum flooding surface (MFS) (cf. Armstrong et al. 2005).

In the studied lower Permian succession, as mentioned above, sediments of the LST of the DS NG 2, 3 and 4 (Figs. 3, 5) represent sediments of several braided streams, suggesting that these deposits may have accumulated in a glaciofluvial setting (see Le Heron et al. 2009). In this glacio-terrestrial setting, deposition occurs on a plain that is characterised by interconnected incisions and braided systems (Duller et al. 2008; Le Heron et al. 2009). These observations are in accordance with our results.

Conclusions

The type section of the Permo−Carboniferous Aheimer Formation in the eastern foot slopes of the Northern Galala Plateau, west of the Gulf of Suez, has been studied by integrating stratigraphical, sedimentological and trace fossil data. Three Permian sequence boundaries (SB1−3) bound four 3rd-order depositional sequences, including the upper Carboniferous DS NG 1, and the lower Permian DS NG 2−4. Litho- and bio- facies development shows a strong relationship to the interpreted sequence architecture. Four different facies associations, comprising 11 facies types, represent a wide spectrum of depositional palaeoenvironments ranging from fluvial, estuarine, intertidal, shallow subtidal, shoreface to offshore transitional settings.

The abundant and diverse late Carboniferous−early Permian ichno-assemblages are composed of horizontal, vertical and sub-vertical traces, confirming the activity of a variety of crustaceans, polychaetes, bivalves and arthropods. At least 26 ichnotaxa have been identified, representing suites of the *Glossifungites*, proximal *Cruziana* and proximal-archetypal *Cruziana* ichnofacies. Ichnofabric analysis revealed three distinct types, including *Tisoa*, *Schaubcylindrichnus* and *Zoophycos* ichnofabrics.

The presence of fully marine trace and body fossils with almost homogeneous distribution supports relatively stable and low-stress conditions. In contrast, the trophic structure of some other assemblages reflects the influence of particular environmental parameters, including substrate consistency, bathymetry, water energy, productivity, rate of sedimentation, salinity and oxygen availability. The integrated results indicate that the sequences were formed during an interval dominated by different perturbations that resulted in a wide spectrum of depositional features. Moreover, evidence for the Carboniferous–Permian glaciation is tentatively established in North Egypt but requires further investigation.

Acknowledgements We are grateful to Chris Boyd (IPC Canada) and an anonymous reviewer for their constructive comments and to the Editor-in-Chief, Maurice Tucker (University of Bristol), for his insightful suggestions that immensely improved the manuscript. We are indebted to Murray Gingras (University of Alberta) for advice, fruitful comments in the early manuscript, and for providing one of us (Magdy El Hedeny) with access to his publication database. Thanks are also due to Anju Saxena (Birbal Sahni Institute of Palaeosciences) for the help with identification of some plant remains. We extend our thanks to Mohamed Rashwan and Mohamed Abdelmaksoud (Alexandria University) for their helps during part of the fieldwork.

Funding Open access funding provided by The Science, Technology & Innovation Funding Authority (STDF) in cooperation with The Egyptian Knowledge Bank (EKB). No funds, grants, or other support was received.

Data availability No supplementary material available for this article.

Declarations

Conflict of interest The authors declare that there is no conflict of interest regarding the publication of this article.

References

Abd El-Azeam S (1990) Geological and stratigraphical studies on the Upper Paleozoic sediments in Wadi Aheimer-Wadi Araba stretch, Gulf of Suez, Egypt. Unpublished PhD thesis, Zagazig University, pp 168

Abdallah AM, Adindani A (1963) Stratigraphy of Upper Paleozoic rocks, western side of the Gulf of Suez. Geol Surv Egypt 25:1–18

Abdel-Fattah ZA, Gingras MK, Caldwell MW, Pemberton SG, MacEachern JA (2016) The *Glossifungites* ichnofacies and sequence stratigraphic analysis: A case study from middle to upper Eocene successions in Fayum, Egypt. Ichnos 23(3–4):157–179. https://doi.org/10.1080/10420940.2016.1185010

Afify AM, Wanas HA, Osman RA, Khater TM (2023) Depositional environments, provenance, paleoclimate, and tectonic setting of the Paleozoic-Lower Mesozoic siliciclastic sedimentary rocks at Um Bogma region, southwestern Sinai, Egypt: facies analysis and geochemistry. Arab J Geosci 16(10):1–34. https://doi.org/10.1007/s12517-022-10979-6

Al Husseini MI (2004) Carboniferous, Permian and Early Triassic Arabian Stratigraphy. GeoArabia Spec Publ 3:221

Algeo TJ, Schwark L, Hower JC (2004) High-resolution geochemistry and sequence stratigraphy of the Hushpuckney Shale (Swope Formation, eastern Kansas): Implications for climato-environmental dynamics of the Late Pennsylvanian Midcontinent Seaway. Chem Geol 206(3–4):259–288. https://doi.org/10.1016/j.chemgeo.2003.12.028

Al-Laboun AA (1987) Unayzah Formation: A new Permian-Carboniferous unit in Saudi Arabia. AAPG Bull 71(1):29–38. https://doi.org/10.1306/94886D3A-1704-11D7-8645000102C1865D

Allen GP, Posamentier HW (1993) Sequence stratigraphy and facies model of an incised valley fill; the Gironde Estuary, France. J Sediment Res 63(3):378–391. https://doi.org/10.1306/D4267B09-2B26-11D7-8648000102C1865D

Al-Youssef W, Ayed H (1992) Evolution of upper Paleozoic sequences and the application of stratigraphy as a tool for hydrocarbons exploration in Syria. 11th Egyptian General Petroleum Corporation Exploration and Production Conference, Cairo, pp. 7–10

Archer AW, Maples CG (1984) Trace-fossil distribution across a marine-to-nonmarine gradient in the Pennsylvanian of southwestern Indiana. J Paleontol 58(2):448–466

Armstrong H, Brasier MD (2005) Microfossils. Blackwell, Malden, p 296

Armstrong HA, Turner BR, Makhlouf IM, Weedon GP, Williams M, Al-Smadi A, Abu Salah A (2005) Origin, sequence stratigraphy and depositional environment of an Upper Ordovician (Hirnantian) deglacial black shale, Jordan. Palaeogeogr Palaeoclimatol Palaeoecol 220(3–4):273–289. https://doi.org/10.1016/j.palaeo.2005.01.007

Awad GH, Said R (1966) Egypt. Lex Stratigr Internat IX Afrique 4b:4–73

Baldwin CT (1977) Internal structures of trilobite trace fossils indicative of an open surface furrow origin. Palaeogeogr Palaeoclimatol Palaeoecol 21(4):273–284. https://doi.org/10.1016/0031-0182(77)90039-6

Bandel K, Kuss J (1987) Depositional environment of the pre-rift sediments - Galala Heights (Gulf of Suez, Egypt). Berl Geowiss Abh A 78:1–48

Bann KL, Fielding CR, MacEachern JA, Tye SC (2004) Differentiation of estuarine and offshore marine deposits using integrated ichnology and sedimentology: Permian Pebbly Beach Formation, Sydney basin, Australia. In: McIlory D (ed) The application of ichnology to palaeoenvironment and stratigraphic analysis. Geolo Soc London Spec Publ 228(1):179–212. https://doi.org/10.1144/GSL.SP.2004.228.01.10

Bellini E, Massa D (1980) A stratigraphic contribution to the Palaeozoic of the southern basins of Libya. In: Salem MJ, Busrewil MT (eds) The Geology of Libya, vol I. Academic Press, London, pp 3–56

Bhattacharya JP, MacEachern JA (2009) Hyperpycnal Rivers and prodeltaic shelves in the Cretaceous seaway of North America. J Sediment Res 79(3–4):184–209. https://doi.org/10.2110/jsr.2009.026

Bischoff B (1968) *Zoophycos*, a polychaete annelid Eocene of Greece. J Paleontol 42(6):1439–1443

Bottjer DJ, Droser ML, Jablonski D (1987) Bathymetric trends in the history of trace fossils. In: Bottjer DJ (ed) New concepts in the use of biogenic sedimentary structures for paleoenuironmental interpretation. SEPM, Pacific Section, Los Angeles, pp 57–65

Bouchemla I, Bendella M, Benyoucef M, Vinn O, Ferré B (2021) *Zoophycos* and related trace fossils from the Chefar El Ahmar Formation, Upper Emsian-Frasnian Ia-Ib (Ougarta, SW Algeria). Proc Geol Assoc 132(2):207–226. https://doi.org/10.1016/j.pgeola.2020.10.010

Boyd C, McIlroy D (2018) The morphology and mode of formation of *Neoeione* igen. nov. from the Carboniferous of northern England. PalZ 92(1):179–190. https://doi.org/10.1007/s12542-017-0379-z

Braakman J, Levell B, Martin J, Potter TL, Van Vliet A (1982) Late palaeozoic gondwana glaciation in Oman. Nature 299:48–50. https://doi.org/10.1038/299048a0

Bradley J (1973) *Zoophycos* and *Umbellula* (Pennatulacea): their synthesis and identity. Palaeogeogr Palaeoclimatol Palaeoecol 13(2):103–128. https://doi.org/10.1016/0031-0182(73)90039-4

Bromley RG (1996) Trace fossils: biology, taphonomy, and applications. Chapman & Hall, London, p 361

Bromley RG, Ekdale AA (1984) *Chondrites*: A trace fossil indicator of anoxia in sediments. Science 224(4651):872–874. https://doi.org/10.1126/science.224.4651.872

Buatois LA, Mángano MG (1993) Trace fossils from a Carboniferous turbiditic lake: Implications for the recognition of additional nonmarine ichnofacies. Ichnos 2(3):237–258. https://doi.org/10.1080/10420949309380098

Buatois LA, Mángano MG (2003) Sedimentary facies, depositional evolution of the Upper Cambrian-Lower Ordovician Santa Rosita Formation in northwest Argentina. J S Am Earth Sci 16(5):343–363. https://doi.org/10.1016/S0895-9811(03)00097-X

Buatois LA, Mángano MG (2011) Ichnology: organism-substrate interactions in space and time. Cambridge University Press, Cambridge, p 358

Buatois LA, Mángano MG, Maples CG, Lanier WP (1998) Ichnology of an Upper Carboniferous fluvio-estuarine paleovalley: The Tonganoxie Sandstone, Buildex Quarry, eastern Kansas, USA. J Paleontol 72(1):152–180. https://doi.org/10.1017/S0022336000024094

Buatois LA, Almond J, Germs GJB (2013) Environmental tolerance and range offset of *Treptichnus pedum*: implications for the recognition of the Ediacaran-Cambrian boundary. Geology 41(4):519–522. https://doi.org/10.1130/G33938.1

Carr ID (2002) Second-order sequence stratigraphy of the Palaeozoic of North Africa. J Petrol Geol 25(3):259–280. https://doi.org/10.1111/j.1747-5457.2002.tb00009.x

Catuneanu O (2006) Principles of sequence stratigraphy. Elsevier, Amsterdam, p 375

Catuneanu O (2017) Sequence stratigraphy: Guidelines for a standard methodology. Stratigraphy and Timescales 2:1–57. https://doi.org/10.1016/bs.sats.2017.07.003

Catuneanu O (2019) Scale in sequence stratigraphy. Mar Pet Geol 106:128–159. https://doi.org/10.1016/j.marpetgeo.2019.04.026

Catuneanu O, Galloway WE, Kendall CGSTC, Miall AD, Posamentier HW, Strasser A, Tucker ME (2011) Sequence stratigraphy: methodology and nomenclature. Newsl Stratigr 44(3):173–245. https://doi.org/10.1127/0078-0421/2011/0011

Chamberlain CK (1971) Morphology and ethology of trace fossils from the Ouachita Mountains, southeast Oklahoma. J Paleontol 4(2):212–246

Clifton HE (2006) A reexamination of facies models for clastic shorelines. In: Posamentier HW, Walker RG (eds) Facies models revisited. SEPM Spec, pp 293−338. https://doi.org/10.2110/pec.06.84.0293

Coe AL (2003) The sedimentary record of sea-level change. Cambridge University Press, Cambridge, p 288

Craig JL, Rizzi C, Said F, Thusu B, Lüning S, Asbali AI, Keeley ML, Bell JF, Durham MJ, Eales MH, Beswetherick S, Hamblett C (2008) Structural styles and prospectivity in the Precambrian and Palaeozoic hydrocarbon systems of north Africa. In: Salem MJ (ed) The Geology of East Libya. Gutenberg Press, Malta, pp 51–122

Crimes TP, Goldring R, Homewood P, Stuijvenberg J, Winkler W (1981) Trace fossil assemblages of deep-sea fan deposits, Gurnigel and Schlieren flysch (Cretaceous-Eocene), Switzerland. Eclogae Geol Helv 74(3):953–995

Dalrymple RW, Knight RJ, Zaitlin BA, Middleton GV (1990) Dynamics and facies model of a macrotidal sand-bar complex, Cobequid Bay—Salmon River Estuary (Bay of Fundy). Sedimentology 37:577–612. https://doi.org/10.1111/j.1365-3091.1990.tb00624.x

Darwish M (1992) Facies developments of the Upper Paleozoic-Lower Cretaceous sequences in the northern Galala Plateau and evidences for their hydrocarbon reservoir potentiality, northern Gulf of Suez, Egypt. Proc 1st Internat Conf Geol Arab World II, Cairo, pp. 175−214

Dasgupta S, Buatois LA (2012) Unusual occurrence and stratigraphic significance of the *Glossifungites* ichnofacies in a submarine paleo-canyon—Example from a Pliocene shelf-edge delta, Southeast Trinidad. Sediment Geol 269–270:69–77. https://doi.org/10.1016/j.sedgeo.2012.06.004

Desai BG, Ippolitov AP, Gulyaev DB (2021) Ichnofabric analysis of transgressive shoreface deposits on the Russian Platform: insight from the Bathonian-Callovian Lukoyanov Formation sands. International Ichnofabric Workshop 16A (virtual) Abstract. Livingston, Alabama, p. 17.

Desjardins PR, Gabriela Mángano M, Buatois LA, Pratt BR (2010) *Skolithos* pipe rock and associated ichnofabrics from the southern Rocky Mountains, Canada: colonization trends and environmental controls in an early Cambrian sand-sheet complex. Lethaia 43(4):507–528. https://doi.org/10.1111/j.1502-3931.2009.00214.x

Droser ML, Bottjer DJ (1986) A semiquantitative field classification of ichnofabric. J Sediment Petrol 56(4):558–559. https://doi.org/10.1306/212F89C2-2B24-11D7-8648000102C1865D

Duke WL, Arnott RWC, Cheel RJ (1991) Shelf sandstones and hummocky cross-stratification: New insights on a stormy debate. Geology 19(6):625–628. https://doi.org/10.1130/0091-7613(1991)019%3c0625:SSAHCS%3e2.3.CO;2

Duller R, Mountney NP, Russell AJ, Cassidy NC (2008) Architectural analysis of a volcaniclastic jökulhlaup deposit, southern Iceland: Sedimentary evidence for supercritical flow. Sedimentology 55:939–964. https://doi.org/10.1111/j.1365-3091.2007.00931.x

Ekdale AA (1985) Paleoecology of the marine endobenthos. Palaeogeogr Palaeoclimatol Palaeoecol 50(1):63–81. https://doi.org/10.1016/S0031-0182(85)80006-7

Ekdale AA, Berger HW (1978) Deep-sea ichnofacies: modern organism traces on and in pelagic carbonates of the western equatorial Pacific. Palaeogeogr Palaeoclimatol Palaeoecol 23:263–278. https://doi.org/10.1016/0031-0182(78)90096-2

Ekdale AA, Mason TR (1988) Characteristic trace-fossil associations in oxygen-poor sedimentary environments. Geology 16(8):720–723. https://doi.org/10.1130/0091-7613(1988)016%3c0720:CTFAIO%3e2.3.CO;2

El-Barkooky AN (1994) Paleozoic−Mesozoic Boundary: its stratigraphical, sedimentological and palaeotectonical implication in Sinai and Gulf of Suez, Egypt. Unpublished PhD thesis, Cairo University, pp 189

El-Noamani ZM, Tahoun SS (2019) First palynological record from the Upper Carboniferous/Lower Permian succession in west Beni Suef Basin, Egypt, with paleoecological and paleogeographical Implications. Egypt J Bot 59(3):779–801. https://doi.org/10.21608/EJBO.2019.10083.1298

El-Sabbagh AM, El-Hedeny M, Al Farraj S (2017) *Thalassinoides* in the middle Miocene succession at Siwa Oasis, northwestern Egypt. Proc Geol Assoc 128:222–233. https://doi.org/10.1016/j.pgeola.2017.01.001

Embry AF (2009) Practical sequence stratigraphy. Canadian Society of Petroleum Geologists, Calgary, p 79

Ernst G, Niebuhr B, Wiese F, Wilmsen M (1996) Facies development, basin dynamics, event correlation and sedimentary cycles in the Upper Cretaceous of selected areas of Germany and Spain. In: Reitner J, Neuweiler F, Gunkel F (eds) Global and regional controls on biogenic sedimentation, II. Cretaceous sedimentation, Research Reports. Göttinger Arbeiten zur Geologie und Paläontologie Sb3, pp 87–100

Eyles N (1993) Earth's glacial record and its tectonic setting. Earth Sci Rev 35(1–2):1–248. https://doi.org/10.1016/0012-8252(93)90002-O

Fabre J (1988) Les séries paléozoıques d'Afrique: une approche. J Afr Earth Sci 7(1):1–40. https://doi.org/10.1016/0899-5362(88)90051-6

Fan RY, Gong YM (2016) Ichnological and sedimentological features of the Hongguleleng Formation (Devonian–Carboniferous transition) from the western Junggar, NW China. Palaeogeogr Palaeoclimatol Palaeoecol 448:207–223. https://doi.org/10.1016/j.palaeo.2015.12.009

Fedonkin MA, Liñán E, Perejón A (1983) Icnofósiles de las rocas precámbrico-cámbricas de la Sierra de Córdoba, España. Bol R Soc Esp Hist Nat Secc Geol 81:125–138

Fekirine B, Abdallah H (1998) Palaeozoic lithofacies correlatives and sequence stratigraphy of the Saharan Platform, Algeria. Geol Soc London Spec Publ 132(1):97–108. https://doi.org/10.1144/GSL.SP.1998.132.01.05

Fillion D, Pickerill RK (1984) Systematic ichnology of the Middle Ordovician Trenton Group, St Lawrence Lowland, eastern Canada. Atl Geol 20(1):1–41. https://doi.org/10.4138/1572

Fillion D, Pickerill RK (1990) Ichnology of the Upper Cambrian? to Lower Ordovician Bell Island and Wabana groups of eastern Newfoundland, Canada. Palaeontogr Can 7:1–183

Florin R (1949) The morphology of *Trichopitys heteromorpha* Saporta, a seed-plant of Palaeozoic age, and the evolution of the female flowers in the Ginkgoinae. Acta Horti Bergiani 15:79–109

Flügel E (2010) Microfacies of carbonate rocks: analysis, interpretation and application. Springer-Verlag, Berlin, p 984

Frey RW, Howard JD (1985) Trace fossils from the Panther Member, Star Point Formation (Upper Cretaceous), Coal Creek Canyon, Utah. J Paleontol 59(2):370–404

Frey RW, Howard JD (1990) Trace fossils and depositional sequences in a clastic shelf setting, Upper Cretaceous of Utah. J Paleontol 64(5):803–820. https://doi.org/10.1017/S0022336000019004

Frey RW, Pemberton SG (1991) The ichnogenus *Schaubcylindrichnus*: morphological, temporal, and environmental significance. Geol Mag 128(6):595–602. https://doi.org/10.1017/S0016756800019713

Frey RW, Seilacher A (1980) Uniformity in marine invertebrate ichnology. Lethaia 13(3):183–207. https://doi.org/10.1111/j.1502-3931.1980.tb00632.x

Fürsich FT, Werner W, Delvene G, García-Ramos JC, Bermúdez-Rochas DD, Piñuela L (2012) Taphonomy and palaeoecology of high-stress benthic associations from the Upper Jurassic of Asturias, northern Spain. Palaeogeogr Palaeoclimatol Palaeoecol 358–360:1–18. https://doi.org/10.1016/j.palaeo.2012.07.006

Gaigalas A, Uchman A (2004) Trace fossils from Upper Pleistocene varved clays S of Kaunas, Lithuania. Geologija 45:16–26

Galloway WE, Hobday DK (1996) Terrigenous clastic depositional systems: applications to petroleum, coa1, and uranium exploration. Springer-Verlag, New York, p 423

Geyer G, Uchman A (1995) Ichnofossil assemblages from the Nama Groip (Neoproterozoic–Lower Cambrian) in Namibia and the Proterozoic-Cambrian boundary problem revisited. Beringeria 2:175–202

Gingras MK, Räsänen ME, Pemberton SG, Romero LP (2002a) Ichnology and sedimentology reveal depositional characteristics of bay-margin parasequences in Miocene Amazonian foreland basin. J Sediment Res 72(6):871–883. https://doi.org/10.1306/052002720871

Gingras MK, Räsänen ME, Ranzi A (2002b) The significance of bioturbated inclined heterolithic stratification in the southern part of the Miocene Solimoes Formation, Rio Acre, Amazonian Brazil. Palaios 17(6):591–601. https://doi.org/10.1669/0883-1351(2002)017%3c0591:TSOBIH%3e2.0.CO;2

Gingras MK, Baniak G, Gordon J et al (2012a) Porosity and permeability in bioturbated sediments. Dev Sedimentol 64:837–868. https://doi.org/10.1016/B978-0-444-53813-0.00027-7

Gingras MK, MacEachern JA, Dashtgard SE (2012b) The potential of trace fossils as tidal indicators in bays and estuaries. Sediment Geol 279(20):97–106. https://doi.org/10.1016/j.sedgeo.2011.05.007

Guiraud R, Bosworth W (1999) Phanerozoic geodynamic evolution of northeastern Africa and the northwestern Arabian platform. Tectonophysics 315(1–4):73–104. https://doi.org/10.1016/S0040-1951(99)00293-0

Guiraud R, Bosworth W, Thierry J, Delplanque A (2005) Phanerozoic geological evolution of Northern and Central Africa: An overview. J Afr Earth Sci 43(1–3):83–143. https://doi.org/10.1016/j.jafrearsci.2005.07.017

Guiraud R, Issawi B, Bosworth W (2001) Phanerozic history of Egypt and surrounding areas. In: Ziegler PA, Cavazza W, Robertson AHF, Crasquin-Soleau S (eds) Peri-Tethys Memoir 6: Peri-Tethyan Rift/Wrench Basins and Passive Margins. Mémoires du Muséum national dHistoire naturelle de Paris 186, pp 469–509.

Gutiérrez-Marco JC, Dronov AV, Knaust D, Lorenzo Álvarez S (2019) Ordovician trace fossils from the upper Tiouririne Formation of Morocco: Preliminary results. 13th International Symposium on the Ordovician System: Contributions of International Symposium. Novosibirsk, Russia, pp 55−57

Gvirtzman G, Weissbrod T (1984) The Hercynian Geanticline of Helez and the Geologic late paleozoic history of the levant the evolution of the Eastern Mediterranean. Geolo Soc London Spec Publ 17:177–186. https://doi.org/10.1144/GSL.SP.1984.017.01.11

Han Y, Pickerill R (1994) *Phycodes templus* isp. Nov. from the Lower Devonian of northwestern New Brunswick, eastern Canada. Atl Geol 30(1):37–46. https://doi.org/10.4138/2118

Harms JC, Southard JB, Walker RG (1982) Structures and sequences in clastic rocks. Tulsa, SEPM, p 851

Hasiotis ST (2012) A brief overview of the diversity and patterns in bioturbation preserved in the Cambrian – Ordovician carbonate and siliciclastic deposits of Laurentia In: Derby JR, Fritz RD, Longacre SA, Morgan WA, Sternbach CA (eds) The great American carbonate bank: The geology and economic resources of the Cambrian–Ordovician Sauk megasequence of Laurentia. AAPG Memoir pp. 111–123. https://doi.org/10.1306/13331491M983457

Hayward BW (1976) Lower Miocene bathyal and submarine canyon ichnocoenoses from Northland, New Zealand. Lethaia 9(2):149–162. https://doi.org/10.1111/j.1502-3931.1976.tb00960.x

Heckel PH (1986) Sea-level curve for Pennsylvanian eustatic marine transgressive-regressive depositional cycles along midcontinent outcrop belt, North America. Geology 14(4):330–334. https://doi.org/10.1130/0091-7613(1986)14%3c330:SCFPEM%3e2.0.CO;2

Heckel PH (1991) Thin widespread Pennsylvanian black shales of Midcontinent North America: A record of a cyclic succession of widespread pycnoclines in a fluctuating epeiric sea Modern and ancient continental shelf anoxia. Geol Soc London Spec Publ 58:259–273. https://doi.org/10.1144/GSL.SP.1991.058.01.17

Herbig HG, Kuss J (1988) The youngest Carboniferous rugose corals from Northern Africa (NE Egypt) - palaeoenvironment and systematics. N Jb Geol Paläont Mh 1:1–22

Hermina M, Wassif A, Tahlawy EIA, Kamel A (1983) The subsurface Palaeozoic section at Wadi Araba, Egypt. Ann Geol Surv Egypt 13:257–269

Höntzsch S, Scheibner C, Kuss J, Marzouk AM, Rasser MW (2011) Tectonically driven carbonate ramp evolution at the southern Tethyan shelf: the Lower Eocene succession of the Galala Mountains, Egypt. Facies 57:51–72. https://doi.org/10.1007/s10347-010-0229-x

Hu B, Qi Y (2000) *Zoophycos* ichnofabric in limestones of the upper carboniferous Taiyuan Formation North China. Coal Geol Explor 28:12–15

Hunter RE, Clifton EH (1982) Cyclic deposits and hummocky cross-stratification of probable storm origin in Upper Cretaceous rocks of the Cape Sebastian area, southwestern Oregon. J Sediment Res 52(1):127–143. https://doi.org/10.1306/212F7EF5-2B24-11D7-8648000102C1865D

Hunter RE, Clifton HE, Phillips RL (1979) Depositional processes, sedimentary structures, and predicted vertical sequences in barred nearshore systems, southern Oregon Coast. J Sediment Res 49(3):711–726. https://doi.org/10.1306/212F7824-2B24-11D7-8648000102C1865D

Issawi B, Jux U (1982) Contributions to the stratigraphy of the Paleozoic rocks in Egypt. Geol Surv Egypt 64:1–28

Issawi B, El-Hinnawi M, Francis M, Mazhar A (1999) The Phanerozoic geology of Egypt: a geodynamic approach. Egypt Geol Surv 76:1–462

Jarvis I, Carson GA, Cooper MKE, Hart MB, Leary PN, Tocher BA, Horne D, Rosenfeld A (1988) Microfossil assemblages and the Cenomanian/Turonian (Late Cretaceous) Oceanic Anoxic Event. Cret Res 9(1):3–103. https://doi.org/10.1016/0195-6671(88)90003-1

Kämpf N, Schwertmann U (1983) Goethite and hematite in a climosequence in southern Brazil and their application in classification of kaolinitic soils. Geoderma 29(1):27–39. https://doi.org/10.1016/0016-7061(83)90028-9

Keeley ML (1989) The Palaeozoic history of the Western Desert of Egypt. Basin Res 2(1):35–48. https://doi.org/10.1111/j.1365-2117.1989.tb00025.x

Klitzsch E (1983) Paleozoic formations and a Carboniferous glaciation from the Gilf Kebir-Abu Ras area in southwestern Egypt. J Afr Earth Sci 1(1):17–19. https://doi.org/10.1016/0899-5362(83)90027-1

Klitzsch E (1990) Palaeozoic. In: Said R (ed) The geology of Egypt. AA Balkema, Rotterdam, pp 393–406

Klitzsch E, Groeschke M, Herrmann-Degen W (1990) Wadi Qena: Paleozoic and pre-Campanian Cretaceous strata. In: Said R (ed) The geology of Egypt. AA Balkema, Rotterdam, pp 321–327

Knaust D (1998) Trace fossils and ichnofabrics on the Lower Muschelkalk carbonate ramp (Triassic) of Germany: tool for high-resolution sequence stratigraphy. Geol Rundsch 87:21–31. https://doi.org/10.1007/s005310050186

Knaust D (2009) Complex behavioural pattern as an aid to identify the producer of *Zoophycos* from the Middle Permian of Oman. Lethaia 42(2):146–154. https://doi.org/10.1111/j.1502-3931.2008.00120.x

Knaust D (2013) The ichnogenus *Rhizocorallium*: Classification, trace makers, palaeoenvironments and evolution. Earth Sci Rev 126:1–47. https://doi.org/10.1016/j.earscirev.2013.04.007

Knaust D (2017) Atlas of trace fossils in well core: appearance, taxonomy and interpretation. Springer, Berlin, p 209

Knaust D (2019) The enigmatic trace fossil *Tisoa* de Serres, 1840. Earth Sci Rev 188:123–147. https://doi.org/10.1016/j.earscirev.2018.11.001

Knaust D (2022) Who were the tracemakers of *Protovirgularia* – Molluscs, arthropods, or annelids? Gondwana Res 111:95–102. https://doi.org/10.1016/j.gr.2022.07.009

Kora M (1984) The Paleozoic outcrops of Um Bogma area, Sinai. Unpublished PhD thesis, Mansoura University, pp 280

Kora M (1998) The Permo-Carboniferous outcrops of the Gulf of Suez region, Egypt: Stratigraphic classification and correlation Peri-Tethys: stratigraphie correlations 2. Geodiversitas 20(4):701–721

Kora M, Mansour Y (1992) Stratigraphy of some Permo-Carboniferous successions in the Northern Galala, Gulf of Suez region, Egypt. N Jb Geol Paläont Abh 185(3):377–394

Kostandi AB (1959) Facies maps for the study of the Palaeozoic and Mesozoic sedimentary basins of the Egyptian region, UAR. 1st Arab Petrol Congr II:54−62

Koutsoukos EAM, Leary PN, Hart MB (1990) Latest Cenomanian-earliest Turonian low-oxygen tolerant benthonic foraminifera: A case study from the Sergipe Basin (NE Brazil) and the western Anglo-Paris Basin (Southern England). Palaeogeogr Palaeoclimat Palaeoecol 77(2):145–177. https://doi.org/10.1016/0031-0182(90)90130-Y

Kureshy AA (1966) Biostratigraphic studies of Chharat and adjacent areas of West Pakistan. Bull Coll Sci 9:85–92

Kuss J, Bachmann M (1996) Cretaceous paleogeography of the Sinai Peninsula and neighbouring areas. CR Acad Sci Paris 322:915–933

Kuss J, Scheibner C, Gietl R (2000) Carbonate platform to basin transition along an Upper Cretaceous to Lower Tertiary Syrian Arc uplift, Galala Plateaus, Eastern Desert, Egypt. GeoArabia 5(3):405–424. https://doi.org/10.2113/geoarabia0503405

Kvale EP, Archer AW (1990) Tidal deposits associated with low-sulfur coals, Brazil Fm. (Lower Pennsylvanian), Indiana. J Sediment Res 60(4):563–574. https://doi.org/10.1306/212F91E7-2B24-11D7-8648000102C1865D

Kvale EP, Archer AW, Johnson HR (1989) Daily, monthly, and yearly tidal cycles within laminated siltstones of the Mansfield Formation (Pennsylvanian) of Indiana. Geology 17(4):365–368. https://doi.org/10.1130/0091-7613(1989)017%3c0365:DMAYTC%3e2.3.CO;2

Le Heron DP, Craig J, Etienne JL (2009) Ancient glaciations and hydrocarbon accumulations in North Africa and the Middle East. Earth Sci Rev 93(3–4):47–76. https://doi.org/10.1016/j.earscirev.2009.02.001

Leckie DA, Walker RG (1982) Storm- and tide-dominated shorelines in Cretaceous Moosebar-Lower Gates interval—Outcrop equivalents of Deep basin gas trap in western Canada. AAPG Bull 66(2):138–157. https://doi.org/10.1306/03B59A53-16D1-11D7-8645000102C1865D

Lejal-Nicol A (1990) Fossil flora. In: Said R (ed) The geology of Egypt. AA Balkema, Rotterdam, pp 615–625

Levell BK, Braakman JH, Rutten KW (1988) Oil-bearing sediments of Gondwana glaciation in Oman. AAPG Bull 72(7):775–796. https://doi.org/10.1306/703C8F29-1707-11D7-8645000102C1865D

Lin HY, Li WH, Lin CF, Wu HR, Zhao YP (2022) International biological flora: *Ginkgo biloba*. J Ecol 110:951–982. https://doi.org/10.1111/1365-2745.13856

Löwemark L, Hong E (2006) *Schaubcylindrichnus formosus* isp. nov. in Miocene Sandstones from Northeastern Taiwan. Ichnos 13:267–276. https://doi.org/10.1080/10420940600843757

Löwemark L, Nara M (2010) Morphology, ethology and taxonomy of the ichnogenus *Schaubcylindrichnus*: Notes for clarification. Palaeogeogr Palaeoclimatol Palaeoecol 297(1):184–187. https://doi.org/10.1016/j.palaeo.2010.07.028

Lüning S, Marzouk AM, Morsi AM, Kuss J (1998) Sequence stratigraphy of the Upper Cretaceous of central-east Sinai, Egypt. Cret Res 19(2):153–196. https://doi.org/10.1006/cres.1997.0104

Lüning S, Craig J, Loydell DK, Storch P, Fitches W (2000) Lowermost Silurian "hot shales" in north Africa and Arabia: regional distribution and depositional model. Earth Sci Rev 49(1–4):121–200. https://doi.org/10.1016/S0012-8252(99)00060-4

MacEachern JA, Burton JA (2000) Firmground *Zoophycos* in the Lower Cretaceous Viking Formation, Alberta: A distal expression of the *Glossifungites* Ichnofacies. Palaios 15(5):387–398. https://doi.org/10.1669/0883-1351(2000)015%3c0387:FZITLC%3e2.0.CO;2

MacEachern JA, Pemberton SG (1992) Ichnological aspects of Cretaceous shoreface successions and shoreface variability in the Western Interior Seaway of North America. In: Pemberton SG (ed) Applications of ichnology to petroleum exploration: A core workshop. SEPM, Tulsa, Core Workshop Notes, pp 57–84. https://doi.org/10.2110/cor.92.01.0057

MacEachern JA, Raychaudhuri I, Pemberton SG (1992a) Stratigraphic applications of the *Glossifungites* Ichnofacies: Delineating

discontinuities in the rock record. In: Pemberton SG (ed) Applications of ichnology to petroleum exploration: A core workshop. SEPM, Tulsa, Core Workshop Notes, pp 169–198. https://doi.org/10.2110/cor.92.01.0169

MacEachern JA, Bechtel DJ, Pemberton SG (1992b) Ichnology and sedimentology of transgressive deposits, transgressively related deposits and transgressive systems tracts in the Viking Formation of Alberta. In: Pemberton SG (ed) Applications of ichnology to petroleum exploration: A core workshop. SEPM, Tulsa, Core Workshop Notes, pp 251–290. https://doi.org/10.2110/cor.92.01.0251

MacEachern JA, Zaitlin BA, Pemberton SG (1999) A sharp-based sandstone of the Viking Formation, Joffre Field, Alberta, Canada: criteria for recognition of transgressively incised shoreface complexes. J Sediment Res 69(4):876–892. https://doi.org/10.2110/jsr.69.876

MacEachern JA, Bann KL, Pemberton SG, Gingras MK (2007a) The Ichnofacies paradigm: High-resolution paleoenvironmental interpretation of the rock record. In: Bann KL, Gingras MK, Pemberton SG (eds) Applied ichnology. SEPM Short Course Notes, Tulsa, pp 27–63. https://doi.org/10.2110/pec.07.52.0027

MacEachern JA, Gingras MK, Bann KL, Pemberton SG, Dafoe LT (2007b) Application of ichnology to high-resolution genetic stratigraphic paradigms. In: MacEachern JA, Bann KL, Gingras MK, Pemberton SG (eds) Applied ichnology. SEPM Short Course Notes, Tusla, pp 93–127. https://doi.org/10.2110/pec.07.52.0095

MacEachern JA, Pemberton SG, Gingras MK, Bann KL (2010) Ichnology and facies models. In: James NP, Dalrymple RW (eds) Facies Models 4. Geological Association of Canada, Canada, pp 19–58

MacEachern JA, Bann KL, Gingras MK, Zonneveld JP, Dashtgard SE, Pemberton SG (2012) The ichnofacies paradigm. In: Knaust D, Bromley R (eds) Trace fossils as indicators of sedimentary environments. Developments in sedimentology, Elsevier, Amsterdam, pp 103–138. https://doi.org/10.1016/B978-0-444-53813-0.00004-6

Mángano MG, Buatois LA, West RR, Maples CG (2002) Ichnology of Pennsylvanian equatorial tidal flat—The Stull Shale Member at Waverly, Eastern Kansas. Kansas Geol Surv Bull 245:1–133

Maurin J-C, Guiraud R (1993) Basement control in the development of the Early Cretaceous West and Central African Rift System. Tectonophysics 228:81–95. https://doi.org/10.1016/0040-1951(93)90215-6

McCann T, Pickerill RK (1988) Flysch trace fossils from the Cretaceous Kodiak Formation of Alaska. J Paleontol 62(3):330–348. https://doi.org/10.1017/S0022336000059138

Meshref WM (1990) Tectonic framework. In: Said R (ed) The geology of Egypt. AA Balkema, Rotterdam, pp 113–155

Miall AD (1985) Architectural-element analysis: A new method of facies analysis applied to fluvial deposits. Earth Sci Rev 22(4):261–308. https://doi.org/10.1016/0012-8252(85)90001-7

Miall AD (1993) The architecture of fluvial-deltaic sequences in the upper Mesaverde Group (Upper Cretaceous), Book Cliffs, Utah. Geol Soc Spec Publ 75:305–332. https://doi.org/10.1144/GSL.SP.1993.075.01.1

Miall AD (1996) The geology of fluvial deposits: sedimentary facies, basin analysis, and petroleum geology. Springer-Verlag, Berlin, p 582

Miller W III (1986) Discovery of trace fossils in Franciscan turbidites. Geology 14:343–345. https://doi.org/10.1130/0091-7613(1986)14%3c343:DOTFIF%3e2.0.CO;2

Miller MF, Knox LW (1985) Biogenic structures and depositional environments of a Lower Pennsylvanian coal-bearing sequence, northern Cumberland Plateau, Tennessee, USA. In: Curran HA (ed) Biogenic structures: Their use in interpreting depositional environments. SEPM Spec Publ, Tusla, pp 67–97

Moustafa AR (2002) Controls on the geometry of transfer zones in the Suez rift and northwest Red Sea: Implications for the structural geometry of rift systems. AAPG Bull 86(6):979–1002. https://doi.org/10.1306/61EEDC06-173E-11D7-8645000102C1865D

Moustafa AR (2013) Fold-related faults in the Syrian Arc belt of northern Egypt. Mar Pet Geol 48:441–454. https://doi.org/10.1016/j.marpetgeo.2013.08.007

Nakkady SE (1955) The stratigraphy and geology of the district between the northern and southern Galala plateaus (Gulf of Suez coast, Egypt). Bull Inst Egypte 36:254–268

Neto de Carvalho C (2006) Roller coaster behaviour in the *Cruziana rugosa* group from Penha Garcia (Portugal): Implications for the feeding program of trilobites. Ichnos 13(4):255–265. https://doi.org/10.1080/10420940600843740

Nummedal D, Swift DJP (1987) Transgressive stratigraphy at sequence-bounding unconformities: Some principles derived from Holocene and Cretaceous examples. In: Nummedal D, Pilkey OH, Howard JD (eds) Sea-level fluctuation and coastal evolution. SEPM Spec Publ, Tusla, pp 241–260. https://doi.org/10.2110/pec.87.41.0241

Omara S (1965) A micropaleontological approach to the stratigraphy of the Carboniferous exposures of the Gulf of Suez region. N Jb Geol Paläont Mh 7:409–419

Omara S, Vangerow F (1965) Carboniferous (Westphalian) foraminifera from Abu Darag Eastern Desert, Egypt. Geol Mijnb 44:87–93

Omran AM, Khalifa H (1988) Microflora (algae, spores and pollen) from Wadi Araba (Eastern Desert, Egypt). Bull Fac Sci Assiut Univ 17(2):1–24

Oschmann W (1993) Environmental oxygen fluctuations and the adaptive response of marine benthic organisms. J Geol Soc 150:187–191. https://doi.org/10.1144/gsjgs.150.1.0187

Osgood RG, Szmuc EJ (1972) The trace fossil *Zoophycos* as an indicator of water depth. Bull Am Paleontol 62(271):5–22

Øygard ØB (2016) A study of the ichnology, lithology and reservoir quality of the Palaeogene Grumantbyen Formation on Svalbard. MSc thesis, University of Bergen, pp 95. https://hdl.handle.net/1956/15426

Patton TL, Moustafa AR, Nelson RA, Abdine SA (1994) Tectonic evaluation and structural setting of the Suez Rift. AAPG Mem 59:7–55. https://doi.org/10.1306/M59582C2

Pemberton SG, Frey RW (1982) Trace fossil nomenclature and the *Planolites-Palaeophycus* dilemma. J Paleontol 56(4):843–881

Pemberton SG, MacEachern JA, Frey RW (1992) Trace fossil facies models: Environmental and allostratigraphic significance. In: Walker RG, James NP (eds) Facies models: Response to sea level change. Geological Association of Canada, Canada, pp 47–72

Pemberton SG, Spilla M, Pulham AJ, Saunders T, MacEachern JA, Robbins D, Sinclair IK (2001) Ichnology and sedimentology of shallow to marginal marine systems: Ben Nevis and Avalon reservoirs, Jeanne d`Arc Basin. St John's, Canada, Geological Association of Canada Short Course Notes, p 343

Plička M (1969) Methods for the study of "*Zoophycos*" and similar fossils. NZ J Geol Geophys 12(2–3):551–573. https://doi.org/10.1080/00288306.1969.10420298

Postma G (1990) Depositional architecture and facies of river and fan deltas: a synthesis. Int Ass Sediment Spec Publ 10:13–27. https://doi.org/10.1002/9781444303858.ch2

Prothero DR, Schwab F (1996) Sedimentary geology. An introduction to sedimentary rocks and stratigraphy. WH Freeman and Company, New York, pp 575

Rafferty JP (2011) The Paleozoic Era: Diversification of plant and animal life. Britannica Educational Publishing, New York, p 339

Raychaudhuri I, Brekke HG, Pemberton SG, MacEachern JA (1992) Depositional facies and trace fossils of a low wave energy shoreface succession, Albian Viking Formation, Chigwell Field, Alberta, Canada. In: Pemberton SG (ed) Applications of ichnology to petroleum exploration: A core workshop. SEPM, Tulsa, Core Workshop Notes, pp 319–337. https://doi.org/10.2110/cor.92.01.0319

Retallack GJ (2001) *Scoyenia* burrows from Ordovician palaeosols of the Juniata Formation in Pennsylvania. Palaeontology 44(2):209–235. https://doi.org/10.1111/1475-4983.00177

Rhoads DC (1967) Biogenic reworking of intertidal and subtidal sediments in Barnstable Harbor and Buzzards Bay, Massachusetts. J Geol 75(4):461–476. https://doi.org/10.1086/627272

Richards MT (1994) Transgression of an estuarine channel and tidal flat complex: The Lower Triassic of Barles, Alpes de Haute Provence, France. Sedimentology 41(1):55–82. https://doi.org/10.1111/j.1365-3091.1994.tb01392.x

Rindsberg AK (1990) Commentary: Ichnological consequences of the 1985 International Code of Zoological Nomenclature. Ichnos 1:59–63. https://doi.org/10.1080/10420949009386333

Rosenthal LRP, Walker RG (1987) Lateral and vertical facies sequences in the Upper Cretaceous Chungo member, Wapiabi Formation, southern Alberta. Can J Earth Sci 24(4):771–783. https://doi.org/10.1139/e87-075

Said R (1962) The geology of Egypt. Elsevier Publication Company, Amsterdam-New York, p 377

Said R (1971) Explanatory notes to accompany the geological map of Egypt. Geol Surv Egypt 56:1–123

Said R (1990) The geology of Egypt. Rotterdam, AA Balkema, p 721

Said R, Eissa RA (1969) Some microfossils from Upper Paleozoic rocks of western coastal plain of Gulf of Suez region, Egypt. Proc 3rd African Micropaleont Coll Cairo, pp. 337−383

Savrda CE (1991) Ichnology in sequence stratigraphic studies: An example from the lower Paleocene of Alabama. Palaios 6(1):39–53. https://doi.org/10.2307/3514952

Savrda CE, Bottjer DJ (1986) Trace-fossil model for reconstruction of paleooxygenation in bottom waters. Geology 14(1):3–6. https://doi.org/10.1130/0091-7613(1986)14%3c3:TMFROP%3e2.0.CO;2

Schweinfurth G (1885) Sur la découverte d'une faune Paléozoique dans le grés d'Egypte. Desert Inst Bull Egypt 6:239–255

Scotese CR (2013) Map Folio 57, Late Pennsylvanian, (301.2, Gzhelian), Paleomap PaleoAtlas for ArcGIS, Late Paleozoic, Paleomap Project, Evanston, IL, vol 4

Seilacher A (1964) Biogenic sedimentary structures. In: Imbrie J, Newell N (eds) Approaches to paleoecology. John Willey and Sons, New York, pp 296–316

Seilacher A (1967a) Bathymetry of trace fossils. Mar Geol 5(5–6):413–428. https://doi.org/10.1016/0025-3227(67)90051-5

Seilacher A (1967b) Fossil behaviour. Sci Am 217(2):72–80

Seilacher A (1970) Arbeitskonzept zur konstruktions-morphologie. Lethaia 3(4):393–396. https://doi.org/10.1111/j.1502-3931.1970.tb00830.x

Seilacher A (2007) Trace fossil analysis. Springer-Verlag, Berlin, p 226

Seilacher A, Hemleben C (1966) Beiträge zur sedimentation und Fossilführung des Hunsrückschiefers. 14. Spurenfauna und Bildungsteife der Hunsrückschiefer (Unterdevon). Notizbl Hess L-Amt Bodenforsch 94:40–53

Seilacher A, Seilacher E (1994) Bivalvian trace fossils a lesson from actuopaleontology. Cour Forsch-Inst Senckenberg 169:5–15

Shahar J (1994) The Syrian arc system: an overview. Palaeogeogr Palaeoclimatol Palaeoecol 112(1–2):125–142. https://doi.org/10.1016/0031-0182(94)90137-6

Sharland PR, Archer R, Casey DM, Davie RB, Hall SH, Heward AP, Horbury AD, Simmons MD (2001) Arabian plate sequence stratigraphy. GeoArabia Spec Publ 2:1–374

Stampfli GM, Borel GD (2002) A plate tectonic model for the Paleozoic and Mesozoic constrained by dynamic plate boundaries and restored synthetic oceanic isochrons. Earth Planet Sci Lett 196(1–2):17–33. https://doi.org/10.1016/S0012-821X(01)00588-X

Stampfli GM, Mosar J, Favre P, Pillevuit A, Vannay J-C (2001) Permo-Mesozoic evolution of the western Tethys realm: the Neo-Tethys East Mediterranean Basin connection. Mém Mus Nat Dhistoire Nat De Paris 186:51–108

Stanley DCA, Pickerill RK (1995) *Arenituba*, a new name for the trace fossil ichnogenus *Micatuba* Chamberlain 1971. J Paleontol 69(3):612–614

Swift DJ (1975) Barrier-island genesis: evidence from the central Atlantic shelf, eastern USA. Sediment Geol 14(1):1–43. https://doi.org/10.1016/0037-0738(75)90015-9

Swift DJP, Figueiredo AG, Freeland GL, Oertel GF (1983) Hummocky cross-stratification and megaripples; a geological double standard? J Sediment Res 53(4):1295–1317. https://doi.org/10.1306/212F8369-2B24-11D7-8648000102C1865D

Swinbanks DD, Luternauer JL (1987) Burrow distribution of thalassinidean shrimp on a Fraser Delta tidal flat British Columbia. J Paleontol 61(2):315–332. https://doi.org/10.1017/S0022336000028493

Toom U, Vinn O, Hints O (2019) Ordovician and Silurian ichnofossils from carbonate facies in Estonia: A collection-based review. Palaeoworld 28(1–2):123–144. https://doi.org/10.1016/j.palwor.2018.07.001

Trewin NH, McNamara KJ (1995) Arthropods invade the land: trace fossils and palaeoenvironments of the Tumblagooda Sandstone (? late Silurian) of Kalbarri, Western Australia. Earth Environ Sci Trans R Soc Edinb 85(3):177–210. https://doi.org/10.1017/S026359330000359X

Tucker ME, Wright VP (1990) Carbonate sedimentology. Blackwell, Oxford, p 482

Uchman A (1995) Taxonomy and palaeoecology of flysch trace fossils: The Marnoso-arenacea Formation and associated facies (Miocene, Northern Apennines, Italy). Beringeria 15:3–115

Uchman A, Rattazzi B (2019) The trace fossil *Circulichnis* as a record of feeding exploration: New data from deep-sea Oligocene-Miocene deposits of northern Italy. CR Palevol 18(1):1–12. https://doi.org/10.1016/j.crpv.2018.05.002

Uchman A, Mikuláš R, Rindsberg AK (2011) Mollusc trace fossils *Ptychoplasma* Fenton and Fenton, 1937 and *Oravaichnium* Plička and Uhrová, 1990: Their type material and ichnospecies. Geobios 44(4):387–397. https://doi.org/10.1016/j.geobios.2010.08.001

Van Wagoner JC, Mitchum RM, Campion KM, Rahmanian VD (1990) Siliciclastic sequence stratigraphy in well logs, cores, and outcrops: Concepts for high-resolution correlation of time and facies. AAPG Methods Explor 7:1–55. https://doi.org/10.1306/Mth7510

Vinn O (2014) *Cruziana* traces from the Late Silurian (Pridoli) carbonate shelf of Saaremaa, Estonia. Est J Earth Sci 63(2):71–75. https://doi.org/10.3176/earth.2014.06

Vinn O, Toom U (2015) The trace fossil *Zoophycos* from the Silurian of Estonia. Est J Earth Sci 64(4):284–288. https://doi.org/10.3176/earth.2015.34

Vinn O, Toom U (2016) Rare arthropod traces from the Ordovician and Silurian of Estonia (*Baltica*). N Jb Geol Paläontol Abh 280(2):135–141. https://doi.org/10.1127/njgpa/2016/0570

Vinn O, Wilson MA (2013) An event bed with abundant *Skolithos* burrows from the late Pridoli (*Silurian*) of Saaremaa (Estonia). Carnets Géol. https://doi.org/10.4267/2042/49316

Vinn O, Bendella M, Benyoucef M, Zhang L-J, Bouchemla I, Ferré B, Lagnaoui A (2020) Abundant *Zoophycos* and *Chondrites* from the Messinian (Upper Miocene) of northwestern Algeria. J Afr

Earth Sci 171:103921. https://doi.org/10.1016/j.jafrearsci.2020.103921

Wennekers JHN, Wallace FK, Abugares YI (1996) The geology and hydrocarbons of the Sirt Basin: a synopsis. In: Salem MJ, Mouzughi AJ, Hammuda OS (eds) The Geology of Sirt Basin. First Symposium on the Sedimentary Basins of Libya, Tripoli, Elsevier, Amsterdam, pp 3–58

Wetzel A, Werner F (1981) Morphology and ecological significance of *Zoophycos* in deep-sea sediments off NW Africa. Palaeogeogr Palaeoclimatol Palaeoecol 32:185–212. https://doi.org/10.1016/0031-0182(80)90040-1

Yurewicz DA (1977) Sedimentology of Mississippian basin-facies carbonates, New Mexico and West Texas—The Rancheria Formation. In: Cook HE, Enos P (eds) Deep-water carbonate environments. SEPM Spec Publ, Tusla, pp 203–219

Zaslavskaya N, Eshet Y, Hirsch F, Weissbrod T, Gvirtzman G (1995) Recycled Lower Paleozoic microfossils (Chitinozoa) in the Carboniferous of Sinai (Egypt) and Permo-Triassic of the Negev (Israel): Paleogeographic considerations. Newsl Stratigr 32(1):57–72. https://doi.org/10.1127/nos/32/1995/57

Zonneveld J-P, Gingras MK, Pemberton SG (2001) Trace fossil assemblages in a Middle Triassic mixed siliciclastic-carbonate marginal marine depositional system. British Columbia. Palaeogeogr Palaeoclimatol Palaeoecol 166(3–4):249–276. https://doi.org/10.1016/S0031-0182(00)00212-1